Geol. Mag. **150** (*3*), *2013, pp. 536–555.* © *Cambridge University Press 2013*
doi:10.1017/S0016756812000702

Volcanism from fissure zones and the Caldeira central volcano of Faial Island, Azores archipelago: geochemical processes in multiple feeding systems

VITTORIO ZANON*†, ULRICH KUEPPERS‡,
JOSÉ MANUEL PACHECO* & INÊS CRUZ§

*Centro de Vulcanologia e Avaliação de Riscos Geológicos, Universidade dos Açores, Ponta Delgada, Portugal
‡Department für Geo- und Umweltwissenschaften, Ludwig-Maximilians-Universität (LMU), Munich, Germany
§Departemento de Geologia and CGUL/IDL, Universidade de Lisboa, Portugal

---

(*Received* 20 December 2011; *accepted* 21 August 2012; *first published online* 3 January 2013)

Abstract – Magmas in Faial Island, Azores (Portugal), were mostly erupted from two fissure zones and the Caldeira central volcano during overlapping periods. The fissure zones follow extensional trends oriented WNW and ESE and erupted nepheline- to hypersthene-normative basalts and hawaiites. The Caldeira central volcano builds the central part of the island, which is cut by the fissure zones. Ne-normative basalts show similar high-field-strength element (HFSE) concentrations but higher large ion lithophile element (LILE) concentrations than hy-normative equivalents. Primitive melts were generated by small (3–5 %) degrees of partial melting of garnet-bearing peridotite, variably enriched in incompatible elements. Overall, basalts from Faial show relatively higher LILE abundances and LILE/HFSE ratios than those of the other islands of the Azores and of many other volcanoes in the Atlantic area. This feature indicates the existence of chemical heterogeneities in the mantle sources characterized by variable degrees of metasomatism, both at local and regional scales. Hawaiites evolved from basalts through 30–40 % fractional crystallization of mafic phases plus some plagioclase, in deep reservoirs, at about 430–425 MPa (∼ 15 km). The Caldeira central volcano rocks range from basalts to trachytes. Basalts, produced under similar conditions as fissure basalts, evolved to trachytes through large degrees of polybaric fractional crystallization (100–760 MPa; i.e. ∼ 3.6–26 km), involving olivine, clinopyroxene, feldspar and minor quantities of amphibole, biotite, apatite and oxides. In contrast, mafic magmas from the fissure zones were erupted directly onto the surface from magma reservoirs mainly located at the crust–mantle boundary.

Keywords: geochemistry, Faial, Azores, mantle heterogeneity, fractional crystallization, fissure volcanism, central volcano.

1. Introduction

Many volcanic systems are characterized by the presence of fissure systems or rifts, radiating from the summit of a central volcano, following local weakness patterns that are linked to the gravitational stress (e.g. Borgia, Ferrari & Pasquaré, 1992; Borgia, 1994; Walter, Klügel & Münn, 2006; Münn, Walter & Klügel, 2006). Magma eruptions from fissure zones or from summit vents in active volcanoes, such as Etna (Italy) and Kilauea (Hawaii, USA), respond to the pressure dynamics of multiple reservoirs (Ryan, Koyanagi & Fiske, 1981; Acocella & Neri, 2003; Corsaro & Pompilio, 2004). Magmas feeding these eruptions are genetically linked to each other by evolution processes occurring in these reservoirs (Garcia *et al.* 2000; Corsaro *et al.* 2009).

In other cases, such as the islands of the Sicily Channel (Italy), some Icelandic volcanoes and the East African Rift, magmas erupted from fissure zones and associated central volcanoes show variable degrees of evolution and are believed to have independent evolution histories and origins (Civile *et al.* 2008; Peccerillo *et al.* 2003, 2007; Lacasse *et al.* 2007). The concurrent emission from different vents of magmas with contrasting compositions, during the same eruption, is interpreted as proof of the simultaneous tapping of distinct magma reservoirs (e.g. Água de Pau Volcano, AD 1563 eruption, Azores; Storey, 1981).

The Island of Faial is located in an area characterized by extensional tectonics (Searle, 1980; Vogt & Jung, 2004). Here, there are two young fissure zones located E and W of a central volcano, respectively (Métrich, Bizouard & Varet, 1981). While the composition of the magmas emitted from the central volcano ranges from basalt to trachyte, the lavas erupted from the fissure zones are basalts to hawaiites. These magmatic suites are geographically well distinguishable from each other and, furthermore, there is no evidence of interaction between them. However, during the 1957–58 eruption, a fracture system, caused by dyke intrusion, propagated from the fissure zone towards the central volcano and ultimately triggered a phreatic explosion inside its caldera (Machado *et al.* 1962).

In this paper, we studied the mineral chemistry as well as major and trace element compositions of

---

† Author for correspondence: vittorio.vz.zanon@azores.gov.pt

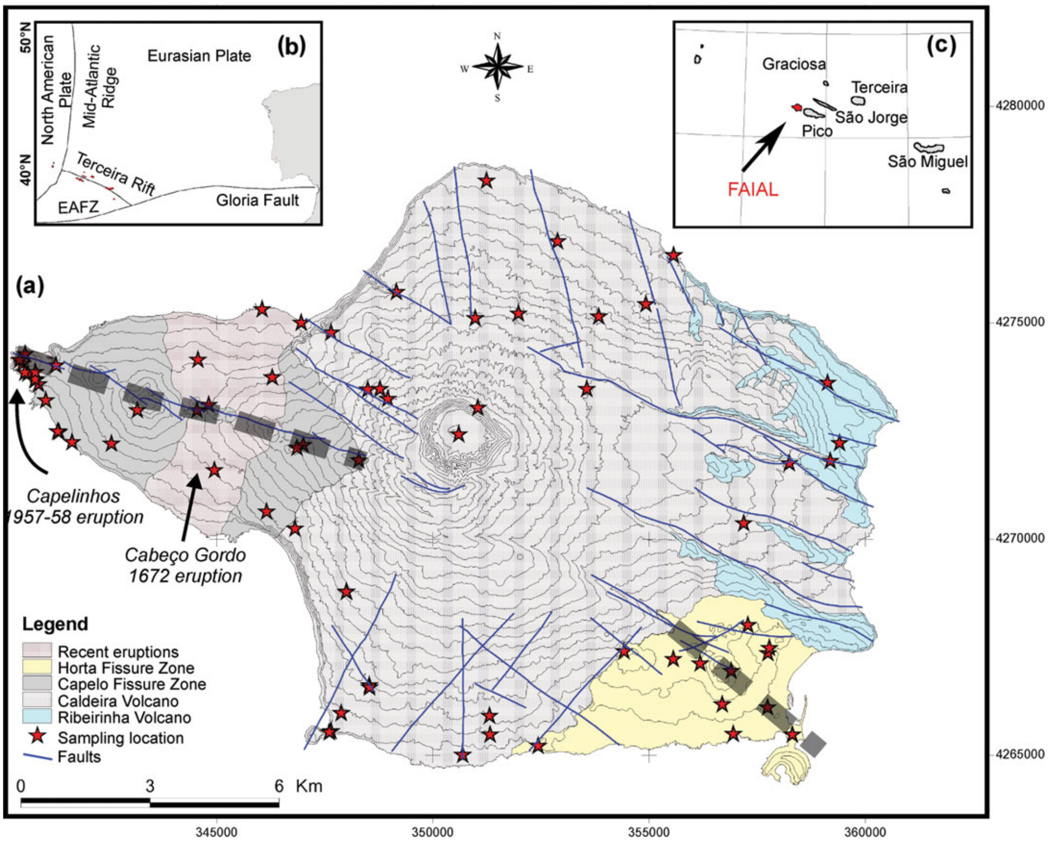

Figure 1. (Colour online) (a) Simplified volcanological map of Faial Island showing the main faults and with sampling locations indicated by red stars. Dashed lines indicate the axis of the two fissure zones. Insets: (b) sketch of tectonic setting; (c) location of Faial Island within the Azores archipelago. EAFZ – East Azores Fracture Zone.

volcanic rocks from the two fissure zones and the central volcano. The main objectives are (i) to define the geochemical characteristics of mafic magmas and the composition of mantle sources beneath Faial as compared to other Azorean volcanoes, (ii) to define the role of differentiation processes during magma ascent and (iii) to provide a model of the plumbing system and the dynamics of magma ascent at Faial.

2. Geodynamic setting and geological history

The nine islands of the Azores archipelago are the emergent portions of large volcanic edifices, which rise from the Azores plateau in the North Atlantic Ocean (Fig. 1b). Magmatism in this area is commonly explained either by the presence of a mantle plume head (e.g. Beier *et al*. 2008 and references therein) or by the melting of a volatile-enriched mantle (Schilling, Bergeron & Evans, 1980; Bonatti, 1990). The archipelago is also subject to intense but low-magnitude seismicity, linked to the interaction among three major tectonic structures: the East Azores Fracture Zone; the transtensional fault system, known as the Terceira Rift; and the Mid-Atlantic Ridge (Searle, 1980; Vogt & Jung, 2004).

Faial is the westernmost island of the central part of the archipelago (Fig. 1c), which rises from a 10–15 Ma crust formed by Mid-Atlantic Ridge eruptions (Müller *et al*. 2008). There are two main tectonic lineaments, with directions WNW–ESE and NNW–SSE (Fig. 1a). The first is the expression of extensional tectonics with normal dextral faults, whereas the latter is a conjugate system constituting a series of transtensional faults on the northern flank of the Caldeira central volcano (Madeira & Silveira, 2003). Recent stratigraphic studies and new K–Ar dates revealed the sequence of the geological events that characterized the history of the island (Hildenbrand *et al*. 2012).

Eruptions took place both from the central volcano and from the fissure zones during the last 1 Ma, in overlapping periods. The oldest rocks, dated back to about 850 ka, crop out in the Pedro Miguel graben (ESE sector) and refer to an older stratovolcano, mostly buried under younger deposits originated from eruptions of the Caldeira Volcano. Nearby, the products of the Ribeirinha Volcano (active from 400 to 350 ka ago) are represented by strongly weathered lava flows dissected by faults. About 120 ka ago, the Caldeira Volcano, in the central part of the island, started its activity that continued until recent times. Two different lithostratigraphic units form this volcano (Pacheco, 2001 and references therein). The Grupo Inferior is formed by lava flows cropping out in the northern and southern coastal cliffs of the island. The Grupo Superior is mostly constituted by pumice fallout deposits produced between about 16 and 1.2 ka ago. During these eruptions a small summit caldera was formed. Eruptions from the Horta Fissure Zone took place in the SE part of the island presumably during the last 11 ka, leading to the formation of a WNW–ESE-oriented basaltic ridge and a lava platform. Eruptions from the Capelo Fissure Zone occurred west of the central volcano in recent times (< 6 ka?; Dias *et al.* 2007), forming a chain of cinder cones and associated lava flows aligned along the WNW–ESE tectonic trend. Two historic eruptions in this area occurred in 1672–73 and 1957–58.

3. Sampling and analytical methods

Eighty-seven samples of lavas and pyroclastic rocks, collected from the four volcanic systems of Faial (Fig. 1a), were chosen for petrographic investigation, and to perform bulk rock and mineral analyses. The largest number of samples comes both from the Capelo (31) and Horta (14) fissure zones and from the Caldeira Volcano (38). Only three samples of the Ribeirinha Volcano were used in this study, owing to limited outcrops and their high degree of weathering.

Electron microprobe analyses were performed making use of a JEOL JXA 8200 Superprobe, equipped with five wavelength-dispersive spectrometers, an energy-dispersive X-ray spectrometer and cathodoluminescence detector, located in the Earth Sciences Department of the ‘Ardito Desio’ University of Milan (Italy). Generally, a spot size of 1 μm with a beam current of 15 nA was utilized, with the exception of biotites and alkali feldspars (5 μm, with a beam current of 5 nA). Glasses were analysed with a current of 2–4 nA and a $\sim$ 10 μm wide defocused beam to minimize sodium loss. Counting times for major elements were 30 s on the peak and 10 s on each background. Natural and synthetic minerals and glasses used as standards were calibrated within 2 % at 2σ standard deviation. Raw data were corrected by applying a Phi-Rho-Z quantitative analysis program. The typical detection limit for each element is 0.01 %. The discrimination between phenocrysts and microphenocrysts was based on the relative crystal size (microphenocryst size is $\sim$150–300 μm, while phenocrysts size is $\geq$ 300 μm).

Whole-rock compositions were obtained at the Activation Laboratories Ltd, Ontario (Canada), after pulverization with an agate ball mill. Rock powders were mixed with a flux of lithium metaborate and lithium tetraborate and fused inside an induction furnace. The melt was then poured into a solution of 5 % nitric acid containing cadmium as an internal standard and continuously stirred until complete dissolution was achieved ($\sim$ 30 minutes). The samples were contemporaneously analysed by means of a Perkin Elmer 9000 inductively coupled plasma mass spectrometer (ICP-MS) and an Agilent 735 inductively coupled plasma atomic emission spectrometer (ICP-AES). FeO was determined by titration with permanganate solution. Three blanks and five controls were analysed per group of samples. Duplicates were fused and analysed every 15 samples. The instruments were recalibrated after 40 samples. Analytical precision (2σ) for trace elements was generally better than 1 % for most major elements and 8 % for most minor and trace elements. Fourteen international rock standards (online Supplementary Data Table S1 available at http://journals.cambridge.org/geo) were used to calibrate the two methods. Whole-rock and mineral compositions are reported in the online Supplementary Data Tables S1 and S2, respectively, at http://journals.cambridge.org/geo.

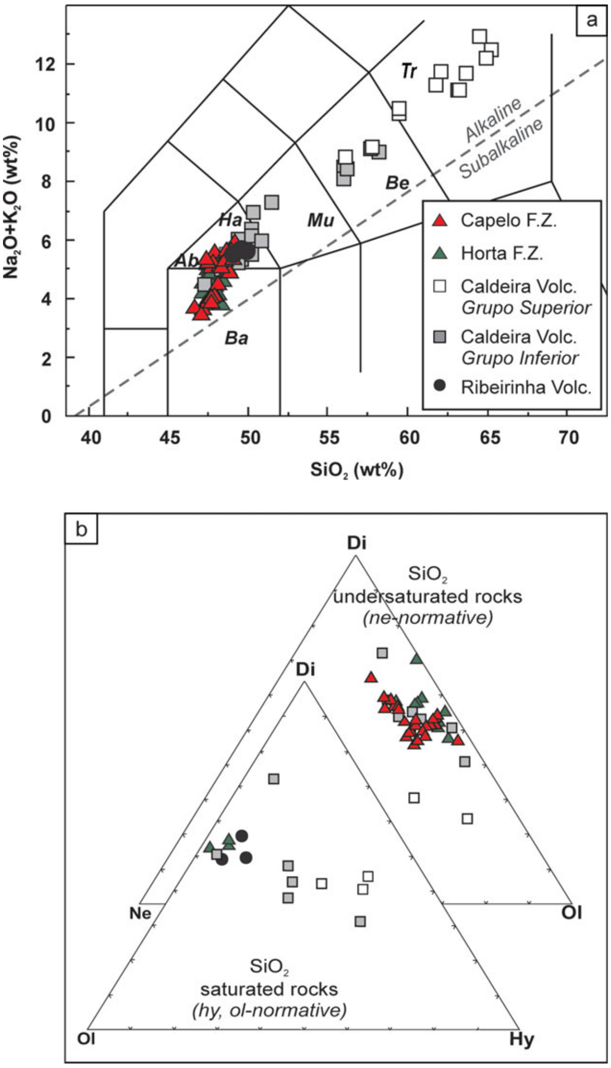

Figure 2. (Colour online) (a) Total Alkali–Silica classification diagram for the rocks of the four volcanic systems in Faial Island. The dotted line indicates the boundary between the alkaline and sub-alkaline series (Macdonald, 1968). Abbreviations: Ba – basalt; Ab – alkaline basalt; Ha – hawaiite; Mu – mugearite; Be – benmoreite; Tr – trachyte. (b) Different silica saturation degrees of the collected samples shown by the use of triangular diagrams of normative mineralogy.

4. Classification, petrography and mineral chemistry

The composition of sampled rocks ranges from basalt to trachyte (Fig. 2a). Basalt and hawaiite are the most abundant rock types, whereas evolved rocks

Table 1. Brief petrographic descriptions and modal analyses of selected samples, representative of the various volcanic systems existing on Faial island

Sample (Cycle)	Long. Lat.	Age	TAS Classification (rock-type)	Mineral assemblage	Modal analysis
FYS341 (RCV)	359485 E 4272187 N	> 580 ka	Hawaiite (lava)	ph: pl + ol micro: ol + pl + ox + cpx gms: pl + ox + ol + cpx	$\mathrm{pl_{21}+ol_{16}+Ti\text{-}mag_{5}+gms_{58}}$
FYS301 (HFZ)	356968 E 4266890 N	< 11 ka	Basalt (lava)	ph: ol + pl micro: pl + ol + ox + cpx gms: pl + cpx + ox	$\mathrm{ol_{8}+pl_{7}+cpx_{1}+(Ti\text{-}mag+ilm)_{6}+gms_{78}}$
FYS302 (HFZ)	356968 E 4266890 N	< 11 ka	Basalt (lava)	ph: ol + cpx + pl micro: pl + ox + ol gms: pl + ol + cpx + ox	$\mathrm{pl_{14}+ ol_{10}+cpx_{8}+(ilm+Ti\text{-}mag)_{7}+gms_{60}}$
FYS328 (HFZ)	357817 E 4266044 N	< 11 ka	Alkali basalt (bomb)	ph: ol micro: pl + ol gms: pl + cpx + ox + gl	$\mathrm{pl_{21}+ol_{10}+Ti\text{-}mag_{3}+gms_{64}}$
FYS327 (CE$_i$)	347681 E 4265496 N	< 410 ka	Benmoreite (lava)	ph: pl + cpx + ap micro: pl + ap + cpx + ol + ox gms: af + cpx + ox + ap + gl	$\mathrm{pl_{28}+ol_{3}+ap_{1}+Ti\text{-}mag_{3}+gms_{66}}$
FYS330 (CE$_i$)	358323 E 4271712 N	< 410 ka	Alkali basalt (lava)	ph: pl + ol + cpx + ox micro: pl + ox + ol + cpx gms: pl + cpx + ox + ol + ap	$\mathrm{pl_{38}+ol_{4}+(Ti\text{-}mag\pm ilm)_{9}+gms_{49}}$
FYS332 (CE$_i$)	359205 E 4273581 N	< 410 ka	Basalt (lava)	ph: pl + ol + cpx micro: pl + ol + ox gms: cpx + pl + ox + ol	$\mathrm{pl_{39}+ol_{2}+cpx_{2}+(Ti\text{-}mag\pm ilm)_{7}+gms_{50}}$
1FA-CE1 (CE$_i$)	355631 E 4276538 N	< 410 ka	Mugearite (lava)	ph: ox + pl micro: pl + cpx + ox gms: pl + af + ox + cpx + ol + gl	$\mathrm{pl_{3}+Ti\text{-}mag_{11}+cpx_{1}+gms_{85}}$
1FA-CE3 (CE$_i$)	355631 E 4276538 N	< 410 ka	Benmoreite (lava)	micro: pl + af + ol + ox gms: af + ox + bt + gl	Rare crystals
2FA-CE (CE$_i$)	349196 E 4275689 N	< 410 ka	Hawaiite (lava)	ph: pl + ox + ol + cpx micro: pl + ol + ox + cpx gms: pl + ol + cpx + ol + gl	$\mathrm{pl_{33}+ol_{7}+Ti\text{-}mag_{7}+gms_{54}}$
FYS321 CE$_s$)	350649 E 4272386 N	< 16 ka	Benmoreite (bomb)	ph: pl + cpx + amp + ox micro: pl + amp + ox + cpx + ol + af gms: pl + ol + ox + amp + gl	$\mathrm{pl_{25}+cpx_{4}+amp_{2}+Ti\text{-}mag_{1}+gms_{68}}$
FYS-14 (CE$_s$)	351029 E 4275077 N	< 16 ka	Trachyte (pumice)	ph: cpx + pl + af + ox + bt micro: bt + af + pl + ap + cpx+ amp gms: bt + ox + ap + gl	$\mathrm{af_{10}+bt_{4}+Ti\text{-}mag_{4}+gms_{82}}$
FYS-17 (CE$_s$)	350739 E 4264943 N	< 16 ka	Trachyte (pumice)	ph: bt gms: bt + ae + gl	Rare crystals
FYS310 (CFZ)	348325 E 4271784 N	< 6 ka	Basalt (lava)	ph: ol + cpx + pl micro: pl + ol + cpx gms: cpx + ox + pl + ol + ap	$\mathrm{pl_{26}+ol_{18}+cpx_{5}+Ti\text{-}mag_{4}+gms_{48}}$
FYS316B (CFZ)	346085 E 4275287 N	< 6 ka	Basalt (lava – ankaramite)	ph: ol + cpx + pl micro: pl + ol + cpx gms: pl + ox + cpx + ol	$\mathrm{pl_{18}+ol_{14}+cpx_{7}+Ti\text{-}mag_{4}+gms_{57}}$
FYS347 (CFZ)	341061 E 4273172 N	< 6 ka	Hawaiite (lava)	ph: pl + ol micro: pl + ol + ox gms: pl + cpx + ol + ox + gl	$\mathrm{pl_{34}+ol_{12}+(Ti\text{-}mag\pm ilm)_{6}+gms_{48}}$
FYS357 (CFZ)	340810 E 4273670 N	AD 1957–58	Alkali basalt (bomb)	ph: ol + cpx micro: pl + ol gms: pl + ol + cpx + ox + gl	
FYS361 (CFZ)	340453 E 4274108 N	AD 1957–58	Alkali basalt (bomb)	ph: cpx + ol micro: pl + ol + cpx gms: cpx + pl + ox + ol + gl	

Mineral abundances are indicated in subscripts and in percentage. Acronyms used: ph – phenocryst, micro – microphenocryst, gms – groundmass, cpx – clinopyroxene, ol – olivine, pl – plagioclase, af – alkali feldspar, amp – amphibole, ae – aegirine, ap – apatite, ilm – ilmenite, Ti-mag – titanomagnetite, ox – oxides (unspecified), bt – biotite, gl – glass.

(mugearite to trachyte) are scarce and mostly owing to eruptions of the Caldeira Volcano in recent times. Trachytic-benmoreitic fall deposits constitute thick covers mantling most of the island topography and severely limit sampling of older rocks.

The investigated samples have a mild Na-alkaline affinity. The samples from the Capelo Fissure Zone are mafic rocks with variable and sometimes very high MgO contents. CIPW norms, calculated using FeO/Fe$_2$O$_3$ ratios according to Irvine & Baragar (1971), indicate that these rocks are all undersaturated in silica with moderate contents in normative nepheline. Horta rocks are also mafic, nepheline- or hypersthene-normative and show less variable MgO contents than the rocks from Capelo. The rocks of the Caldeira Volcano are more evolved (MgO $\leq$ 4.4 wt %), ne- to hy-normative and become quartz-normative in trachytes (qz $\leq$ 3.6 %). The few Ribeirinha samples are hawaiites and are hy-normative (hy = 1.6–3.2 %) (Fig. 2b). A brief petrographic description of the most representative samples for all volcanic systems is reported in Table 1.

4.a. Ribeirinha Volcano

All rocks sampled from this volcano are lavas showing a porphyritic texture both at the meso- and micro-scale. Total phenocryst content is about 30–40 vol. %, constituted by plagioclase, olivine and rare clinopyroxene, with Fe-Ti oxides as accessory phases. The groundmass is intersertal to intergranular.

Plagioclase phenocrysts are dominant, typically tabular, euhedral or subhedral; less commonly they are euhedral and acicular. The largest crystals are antecrysts (Davidson *et al.* 2007) and show disequilibrium features (rounded shape, embayments, anhedral melt inclusions at rims and strong rim zoning). Microphenocrysts in the matrix are euhedral and their composition shows a limited variability (An_{58-63}, Ab_{36-41}, Or_{1-2}). In addition, the groundmass plagioclase is compositionally homogeneous (An_{48-50}, Ab_{48-50}, Or_2) (Fig. 3a). Many olivine phenocrysts and microphenocrysts (9–16 vol. %) show hopper or more rarely swallow-tail and hourglass morphologies (Donaldson, 1976). Euhedral crystals show 10 to 30 μm thick iddingsitic films at their rims and along cracks. Their composition ranges from Fo_{72} to Fo_{80}, while the groundmass composition is constant (Fo_{72}). Augite clinopyroxenes (Wo_{43-45}, En_{41-43}, Fs_{13-16}) are found only in the groundmass. Highly resorbed phenocrysts and anhedral microphenocrysts are rarely observed. Fe-Ti oxides (from Usp_{43} to Usp_{49}) are ubiquitous in all samples as euhedral microphenocrysts in the matrix and as inclusions in olivines. Subhedral and/or anhedral ilmenite is also present in some samples. Apatite is in the groundmass.

4.b. Caldeira Volcano

Sampled lavas range from aphyric to porphyritic (total phenocryst content 0–40 %) hypocrystalline, and contain feldspar, olivine, clinopyroxene and amphibole in decreasing amounts, set in an intergranular, pilotaxitic to doleritic groundmass. Most of the mafic rocks show variably porphyritic textures with plagioclase (up to 39 %) predominating over other phases. Some other mafic rocks are almost aphyric with moderate amounts of microphenocrysts set in a micro- to cryptocrystalline groundmass. Pumices are hypocrystalline, aphyric to scarcely porphyritic (total crystal content $\leq$ 18 %), with phenocrysts of plagioclase predominating over anorthoclase and sanidine, clinopyroxene (both augite and aegirine), amphibole and biotite. Pumices are typically banded, both at a meso- and micro-scale.

Plagioclase phenocrysts are euhedral, tabular, twinned and show oscillatory to normal zoning and embayments. Phenocryst and microphenocryst compositions from various samples with different degrees of evolution show a continuous trend from bytownite to andesine (An_{83-30}, Ab_{17-66}, $Or_{0.4-4}$) in Figure 3a. In some pumices, plagioclase phenocrysts show resorption, indicating disequilibrium with the surrounding melt. Alkali feldspar (anorthoclase and Na-sanidine) is also present as euhedral, tabular and zoned phenocrysts or microphenocrysts in pumices and in some of the lavas (modal abundance < 10 vol. %). Many crystals in the pumices are antecrysts, showing evident resorption. Pyroxene appears as small anhedral and partly resorbed crystals with embayments and reaction rims. Its core compositions range from diopside and diopside-augite in lavas to augite in pumices (Wo_{42-48}, En_{36-43}, Fs_{12-19}) (Fig. 3b). Aegirine-augite crystals are found in a few pumice samples. Euhedral magnetites (Usp_{48-83}) and subhedral ilmenites (Fig. 3c) are commonly found as microphenocrysts. Fluorapatite ($Cl < 0.3$ wt %, $F >$ 2 wt %), kaersutite amphibole and biotite are present in many evolved samples as both phenocrysts and microlites in the matrix. Quartz is present in many trachytic pumices.

4.c. Horta and Capelo fissure zones

Most of the rocks erupted from the Horta and Capelo fissure zones range from sub-aphyric (Fig. 4a) to porphyritic (Fig. 4b). A group of mafic rocks from the Capelo Fissure Zone shows porphyritic textures with up to 30–50 % of large (up to 1 cm) phenocrysts of olivine, clinopyroxene and rare plagioclase, set in a microcrystalline to cryptocrystalline groundmass. Some large crystals show resorbed rims and embayments, indicating disequilibrium with the surrounding melt, and providing evidence for an antecrystic origin (Fig. 4c). These samples will be referred to as ankaramites. Other mafic samples are moderately porphyritic with euhedral clinopyroxene, plagioclase and olivine microphenocrysts set in a micro- to cryptocrystalline groundmass made of the same phases plus Fe-Ti oxides and some glass. Glomeroporphyritic aggregates of clinopyroxene + plagioclase ± olivine ± titanomagnetite are sometimes present.

Bytownite plagioclase is common in all samples as euhedral phenocrysts showing normal or oscillatory zoning and albite twinning. Labradorite is found in the groundmass as small acicular crystals. Olivine is common and occurs as rounded antecrysts in the ankaramites and as phenocrysts and groundmass phase in all mafic samples. Phenocrysts are generally euhedral/subhedral with polyhedral or granular morphology and hopper and swallow-tail morphologies in only minor amounts. Phenocryst composition (Fo_{72-86}) is more Fo-rich than the groundmass (Fo_{63-76}). Clinopyroxene occurs as large resorbed crystals with small embayments and normal to oscillatory zoning, mainly in the strongly porphyritic ankaramites, and as phenocrysts in most of the analysed samples. Composition is diopside to augite (Wo_{43-49}, En_{37-45}, Fs_{10-17}), sometimes with aegirine-augite rims. Clinopyroxene megacrysts in the most MgO-rich ankaramite of the Capelo Fissure Zone have lower contents of Ti and Ca and higher contents of Mg and Al^{VI} than other clinopyroxenes. The variations of the Al^{IV}/Al^{VI} ratio and Ti in clinopyroxenes of the central volcano and the Capelo Fissure Zone are negatively correlated with

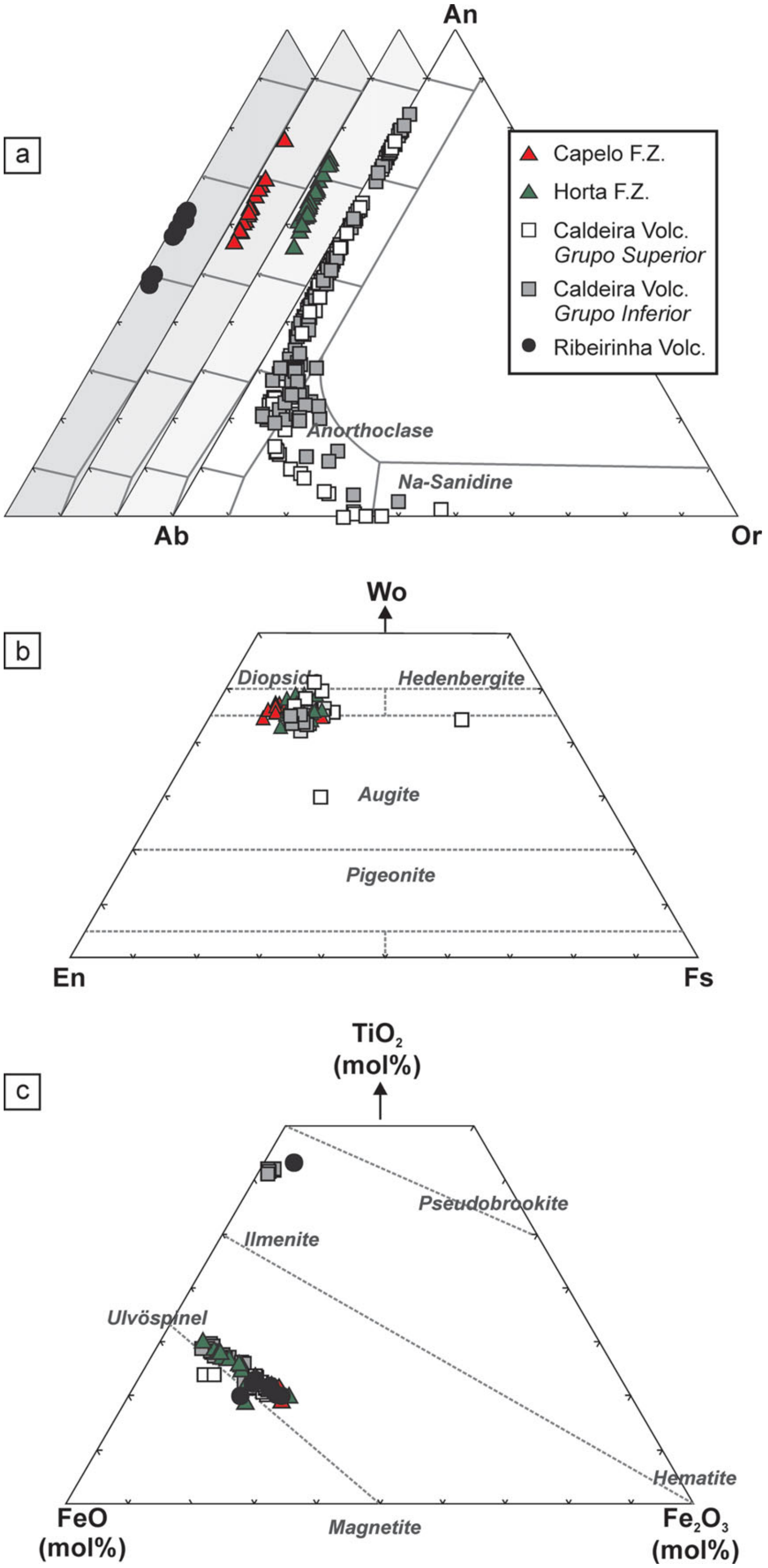

Figure 3. (Colour online) (a) Ternary feldspar diagram with microprobe compositions from phenocrysts, microphenocrysts and groundmass from the four volcanic areas. (b) Classification diagram of clinopyroxenes (Morimoto, 1989). (c) Triangular classification diagram of Fe-Ti oxides.

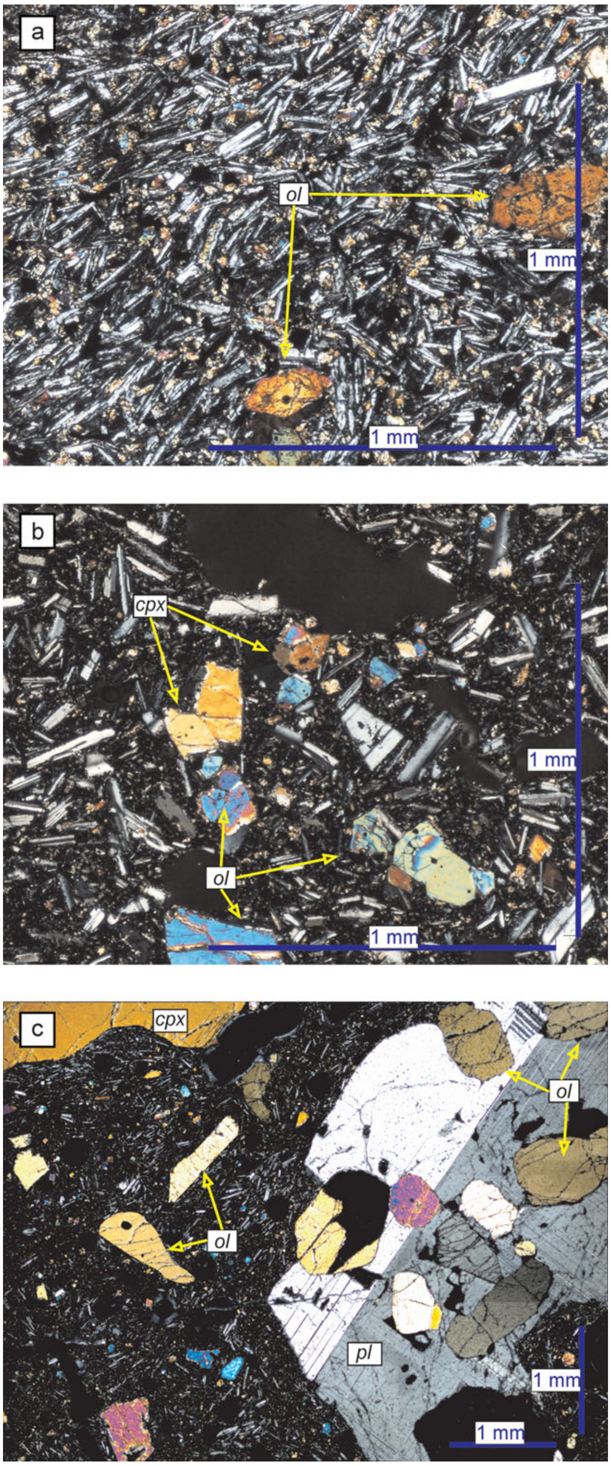

Figure 4. (Colour online) Textures of representative mafic rocks from Faial Island. (a) Sub-aphyric FYS301 basalt from the Horta Fissure Zone. (b) Porphyritic FYS361 basalt from the Capelo Fissure Zone showing evidence for the presence of numerous euhedral plagioclase and a few mafic phases. (c) Highly porphyritic FYS316b ankaramite from the Capelo Fissure Zone. Abbreviations: cpx – clinopyroxene; ol – olivine; pl – plagioclase.

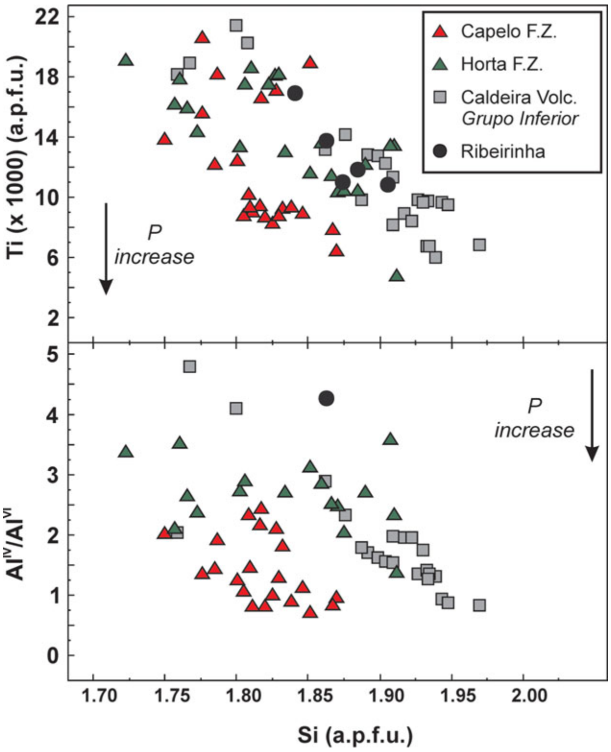

Figure 5. (Colour online) Relative variations of Si, Ti and Al^{IV}/Al^{VI} ratio atomic proportions in clinopyroxene from Faial volcanic systems. The decrease in Ti and Al^{IV}/Al^{VI} ratio with increasing Si is directly related to increasing pressure (Wass, 1979). Abbreviations: a.p.f.u. – atoms per formula unit.

Si and form distinct trends (Fig. 5). According to Wass (1979), these negative trends are related to the variation of the crystallization pressure. In contrast, data from the Horta Fissure Zone are scattered and mostly show high and poorly variable Al^{IV}/Al^{VI} and a more pronounced variation in Si, as compared to the other volcanic systems. Fe-Ti oxides (1–9 vol. %) are common in all samples as euhedral crystals (Usp$_{41–83}$) and as grains in the groundmass. Ilmenite forms subhedral acicular crystals and is also present in the groundmass together with titanomagnetite (Fig. 3c). Euhedral and small-size Cr-spinels occur embedded in many olivine antecrysts and phenocrysts.

5. Geochemistry

Variations in major elements versus MgO indicate an overall continuous variation from mafic to felsic rocks (Fig. 6), with a significant scattering of some elements for the intermediate samples (MgO = 2–4 wt %). A clear kink in the variation trend of some major oxides is observed at MgO values of 4 wt %.

The rocks from the Capelo and Horta fissure zones show large variations in MgO (between 5.2 and 12.5 wt %), with highly porphyritic ankaramites displaying MgO > 10 wt %. There is a small increase in CaO and a decrease in most other major elements with increasing MgO, all defining smooth trends. FeO$_{total}$ is almost constant. For MgO contents of 6–8 wt %, Capelo basalts show slightly higher values of Na$_2$O and K$_2$O (respective average 3.6 and 1.6 wt %) than those of Horta (respective average 3.4 and 1.5 wt %). Caldeira rocks show lower MgO contents as well as different variation trends to Horta and Capelo. Silica and TiO$_2$ show a small compositional gap between mugearites

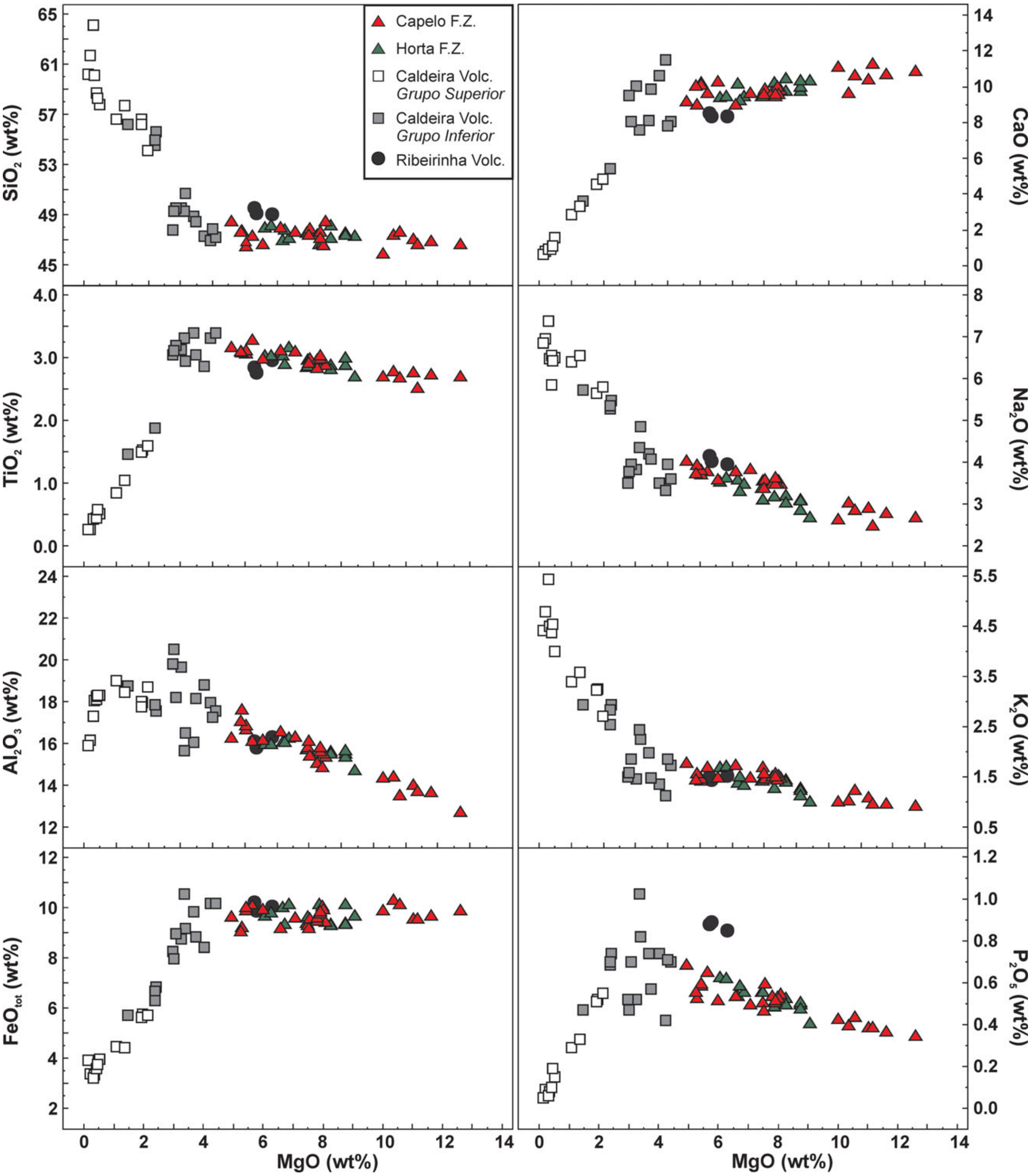

Figure 6. (Colour online) Variation diagrams of major elements v. MgO.

and benmoreites, which might depend on the lack of exposure of intermediate rocks in the field, owing to the large post-16 ka pyroclastic cover.

The few Ribeirinha Volcano lava compositions show limited variations in MgO content (5.7–6.3 wt %). They show slightly higher P_2O_5, Na_2O, SiO_2 and lower CaO contents than samples of the younger fissure zones at the same MgO content.

Compatible elements such as Ni, Sc, Cr and Co show positive correlation with MgO, whereas large ion lithophile elements (LILE: Rb, Ba, K, Cs) and high-field-strength elements (HFSE: Ta, Nb, Zr, Hf, Th, U) have opposite trends (Fig. 7). Barium and Sr increase with decreasing MgO content in mafic and intermediate samples, and decrease in the trachytes of the Caldeira Volcano. Two highly porphyritic benmoreites have an anomalously high Ba content and fall outside the trend defined by the bulk of the samples. A group of trachytes appears strongly enriched in incompatible elements (Rb, U, Th and rare earth elements) and depleted in Sr, as compared to other trachytes that have similar major element compositions. At the same MgO content (8–

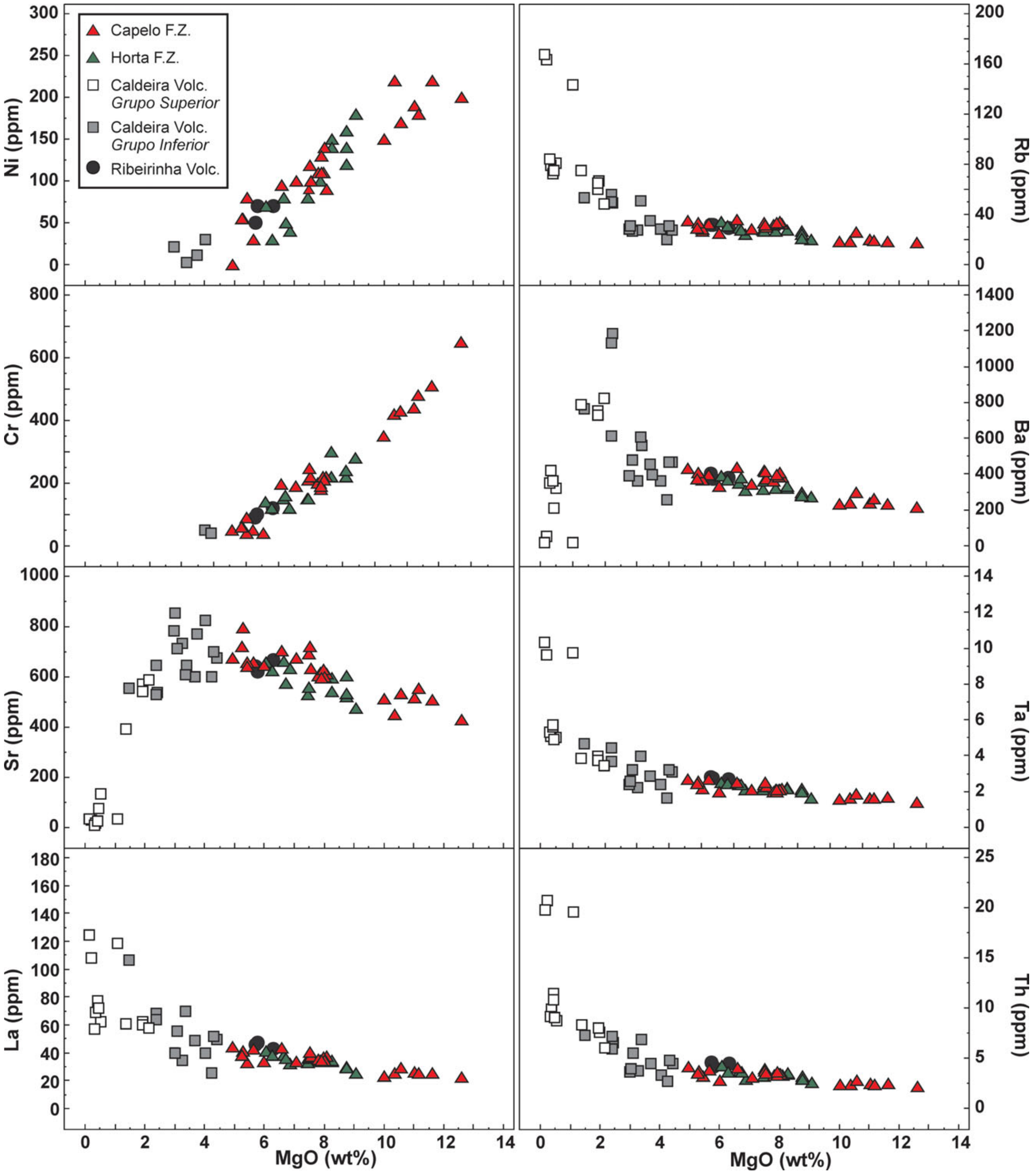

Figure 7. (Colour online) Variation diagrams of selected trace elements v. MgO.

6 wt %), Capelo basalts show slightly higher Sr, Rb and Ba and lower heavy rare earth element (HREE) contents as compared to those from Horta.

Mantle-normalized multi-element patterns (Fig. 8) from basalts to mugearites from all the volcanic systems are very similar to one another and show a smooth upward convex shape with small anomalies in K, Hf and Pb (when detected), which are more remarkable in samples from Caldeira. Patterns for the evolved rocks show negative spikes in Ba, Sr and Ti. REEs are moderately fractionated for both light and heavy elements in all the mafic rocks (not shown). Benmoreites to trachytes display poorly fractionated HREE patterns and sometimes negative Eu anomalies.

6. Thermobarometry calculations

Thermobarometric data, reported in Table 2, were calculated to obtain information on the physical conditions of magma storage and crystallization. Regarding the temperature calculation, we used,

https://doi.org/10.1017/S0016756812000702

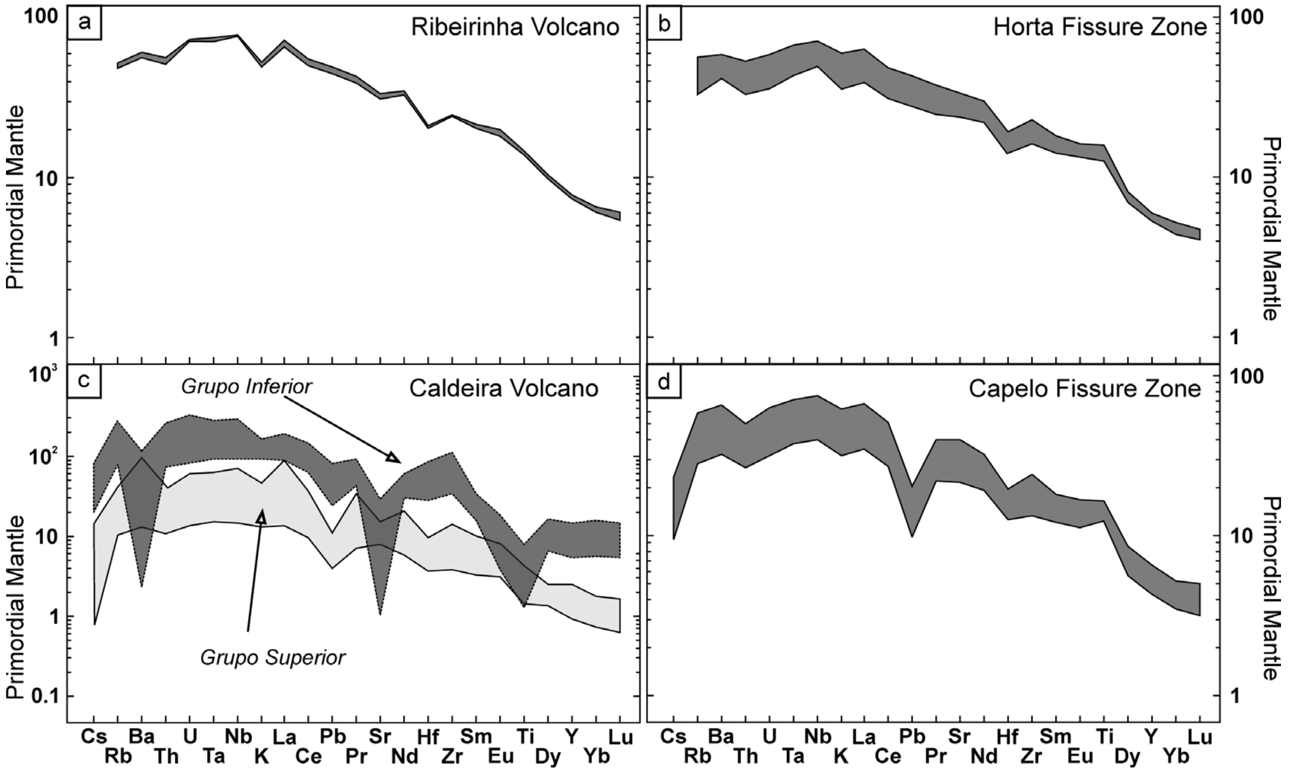

Figure 8. Primordial-mantle-normalized diagrams of incompatible elements (McDonough & Sun, 1995).

Table 2. Geothermobarometry and oxygen fugacity data of Faial volcanic rock compositions

Volcanic system	Compositional range	T (°C)	Ref	P (Mpa)	Ref	Depth (km)	fO_2	Ref.
Capelo	ankaramite	1270 ± 7	(c)	1016	(c)	33.8		
		1106 ± 28	(c)*	858 ± 105	(c)*	28.8		
				476 ± 20	(c)*	16.7		
Capelo and Horta	Hy or Ne-normative basalt–alkali basalt	1155 ± 34	(c)	687 ± 78	(c)	23.4	−4.61 ± 0.35	(b)
		1040 ± 18	(c)*	499 ± 29	(c)*	17.4	−5.7 ± 0.3 (NNO)	
Capelo and Horta	Ne-normative hawaiite	1009 ± 33	(c)	425 ± 15	(c)	15.1	−5.2 and −6.6 ± 0.8 (NNO)	(b)
Ribeirinha	hawaiite	1018 ± 15	(c)*	430 ± 131	(c)*	15.3	−11.99 (MnMnO)	(a)
Caldeira	Hy-normative basalt–hawaiite	1056–1100 ± 30	(b)	760 ± 90	(b)	25.7	−14.21 (QFM)	(b)
		986 ± 23	(c)	421 ± 15	(c)	15.0	−12.93 (NNO)	
Caldeira	High Sr benmoreite	970 ± 19	(c)	159 ± 32	(c)	9.2		
		946 ± 8	(c)					
		982 ± 23	(c)†					
		991 ± 34	(c)†					
		993 ± 31	(c)†					
		1009 ± 18	(c)†					
		1111 ± 21	(c)†					
Caldeira	High Sr trachyte	953 ± 22	(d)	100 ± 47	(c)*	3.6		
				132 ± 15	(c)*	4.8		

Data are calculated either based upon the chemical composition of clinopyroxene or upon the clinopyroxene-liquid equilibrium (*), or upon plagioclase-liquid equilibrium (†). In a single case, the condition of equilibration of various coexisting phases was calculated by the use of QUILF software, while temperatures for trachytes were calculated using the thermometer based upon the chemical composition of amphibole. References are: (a) Andersen & Lindsley (1985); (b) Andersen, Lindsley & Davidson (1993); (c) Putirka (2008); (d) Ridolfi & Renzulli (2012).

whenever possible, the composition of groundmass glass and of the coexisting mineral phases, either plagioclase or clinopyroxene (Putirka, 2008). However, despite the large mineral database, these conditions were rarely met. For this reason, we used alternative algorithms that consider either the equilibrium among clinopyroxene–olivine–spinel–ilmenite (Andersen, Lindsley & Davidson, 1993), or solely focus on the chemical composition of the clinopyroxenes (Putirka, 2008). The presence of amphibole in the evolved magmas allowed the use of a recently developed thermometer based upon the chemical composition of amphibole (Ridolfi & Renzulli, 2012). Although it was calibrated for calcic amphibole, it was also proven quite reliable for alkaline amphibole.

However, since the algorithm involving only the composition of the clinopyroxene is quite imprecise, and owing to the diffuse presence of antecrysts, we extrapolated the temperature path by comparing all available temperature estimations with the MgO content in the bulk rocks. With the exception of a few outliers (antecrystic clinopyroxenes), a good correlation was found ($R^2 = 0.98$), suggesting the existence of a single liquid line of descent, common to all the volcanic series. For this reason, we considered these temperatures fully representative of the conditions of crystallization of the Faial magmas. The use of these temperatures in the clinopyroxene-liquid barometer provided reliable calculations of pressure values (Putirka, 2008).

7. Discussion

7.a. Nature of the magma source and characteristics of primitive melts

The geochemistry of the source regions beneath the Azores archipelago has been widely discussed during the last two decades to reveal the existence of considerable differences in the Sr–Nd–Pb isotopic signature. In particular, four isotopically distinct end-members have been recognized (Millet *et al.* 2009; Beier, Haase & Turner, 2012). These are represented by the high $^{206}Pb/^{204}Pb$, high $^{87}Sr/^{86}Sr$ magmas from São Miguel Island, the high $^{206}Pb/^{204}Pb$, low $^{87}Sr/^{86}Sr$ magmas from Graciosa, Terceira and São Jorge islands, and by the low $^{206}Pb/^{204}Pb$, low $^{87}Sr/^{86}Sr$ magmas from Faial Island and the western part of Pico Island. A fourth component, present in most of the islands, can be found at the intersection of the compositional field of São Miguel with that of Terceira, and is thought to consist of upper mantle material from the nearby Mid-Atlantic Ridge (Turner *et al.* 1997; Moreira *et al.* 1999; Millet *et al.* 2009).

The most common explanation for this large variety of end-members refers to a mixing process at the regional scale between enriched and depleted mantle types (França *et al.* 2006; Millet *et al.* 2009). Enriched mantle types (EM-I, EM-II and HIMU end-members) show an important ‘crustal signature’, which is thought to be the result of either melting of a deep-seated eclogitic crust, related to subduction processes older than 2.5 billion years (Turner *et al.* 2007), or of contamination/assimilation with recycled basaltic material (Widom & Shirley, 1996; Beier, Stracke & Haase, 2007; Elliott *et al.* 2007). The depleted mid-ocean ridge basalt (MORB) mantle (or DMM) is the source for MORB, and uncontaminated by enriched components.

While the isotopic compositions of the easternmost islands, São Miguel and Terceira islands, indicate interaction between EM-II and HIMU end-members (Beier, Haase & Hansteen, 2006; Elliott *et al.* 2007), lavas erupted on the islands of the central part of the archipelago, São Jorge and especially Pico, which is only a few kilometres from Faial, indicate possible mixing among DMM and EM-I end-members. The Sr–Nd–Pb fields of the basalts of Faial Island overlap with the least $^{206}Pb/^{204}Pb$ radiogenic compositions of Pico Island; however, Faial basalts show more radiogenic Sr isotopic compositions. The EM-I type signature of some Faial–Pico magmas is associated with very low $^{187}Os/^{188}Os$ ratios that are typical of unradiogenic reservoirs and suggest the presence of material from an ancient subducted oceanic plate (Schaefer *et al.* 2002; Turner *et al.* 2007). On the other hand, the depleted signatures of other samples from Faial match with the short distance of this island from the Mid-Atlantic Ridge (~ 100 km), suggesting that these magmas suffered extensive mixing with MORB melts (Millet *et al.* 2009).

To unravel the melting processes and the composition of the source rocks for the Faial magmas it is necessary, however, to investigate the geochemical characteristics of the primitive (i.e. poorly evolved) mafic rocks, which are commonly found at both the Capelo and Horta fissure zones. These rocks are aphyric-to-sub-aphyric at the hand specimen scale and reveal a poorly porphyritic texture under the microscope, with small amounts of euhedral microphenocrysts (~ 5 to 15 vol. %). The compositional range of these rocks spans from saturated (hy-normative) to slightly undersaturated (ne-normative) in silica (Fig. 2b) and, in addition, they have lower contents of MgO (~ 9–7 wt %), Ni (~ 80–150 ppm) and Cr (~ 100–300 ppm), as well as Mg no. (~ 55–65), than mantle-equilibrated melts. They can be assumed to be derivative liquids of primary melts that underwent moderate degrees of fractional crystallization of mafic phases, especially olivine with accessory spinel. These processes significantly modified compatible element abundances such as Ni and Cr, but caused a minor enrichment in incompatible elements, while leaving incompatible element ratios unaffected. Therefore, incompatible trace element ratios and, to a lesser extent, their abundances can be used in these samples to constrain the composition of primary magmas and mantle melting processes.

The variable degrees of silica saturation and LILE abundances of the Faial basalts can be explained by the assumption that they are related to each other by high-pressure fractional crystallization processes (O’Hara, 1968; Green & Ringwood, 1976; Gupta, Green & Taylor, 1987). However, similar abundances of MgO, Ni and Cr (Fig. 7) argue against this hypothesis, and the variable pristine composition of the primary melts is considered to be a better explanation.

These basalts show low variability of some elements, especially HFSEs (Fig. 7) and some element ratios

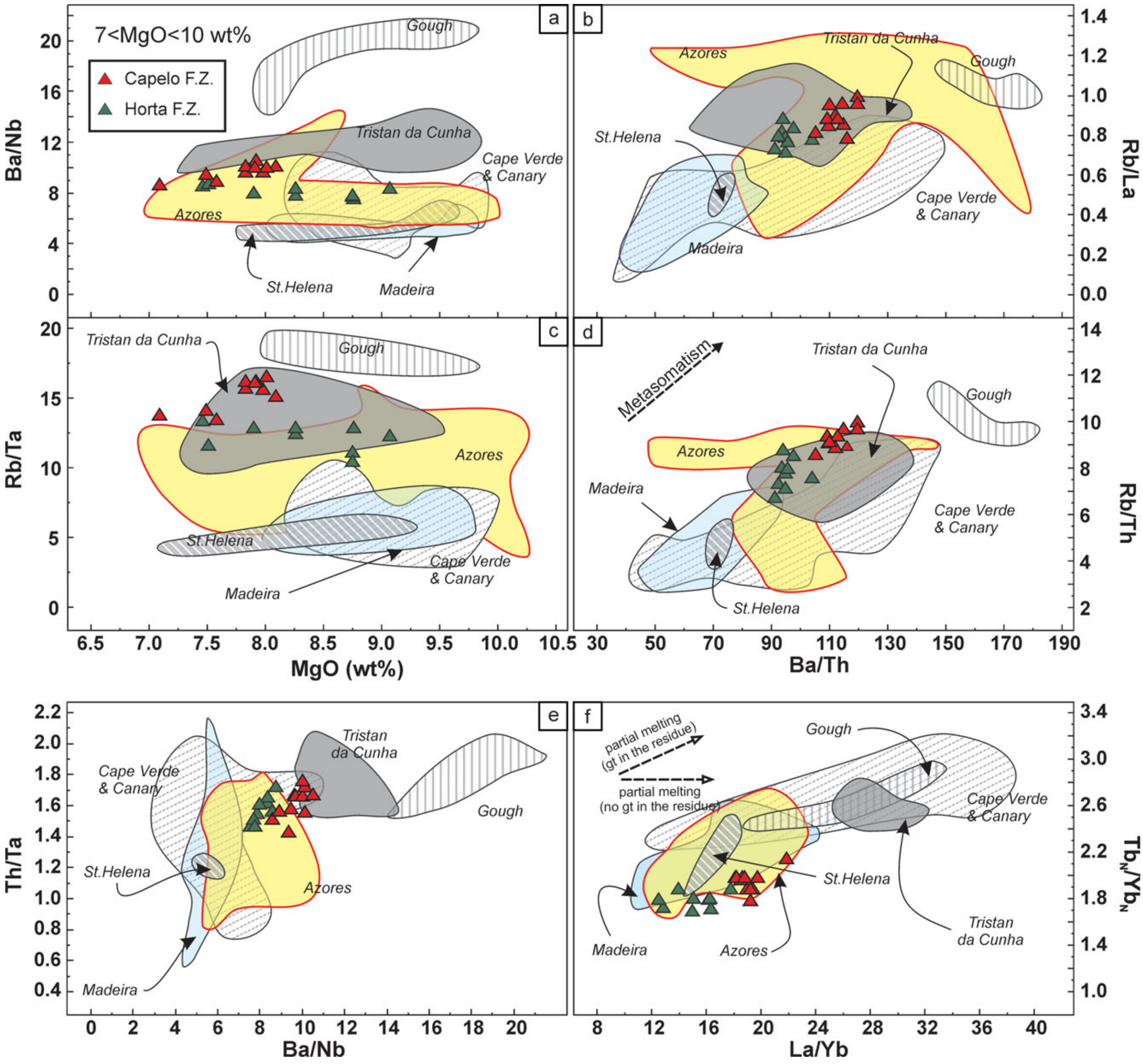

Figure 9. (Colour online) Variations of selected trace element ratios of Faial primitive magmas ($7 < \text{MgO} < 10$ wt %) of both the Horta and Capelo fissure zones. Fields of compositionally similar mafic rocks (MgO range and alkali content) from other islands of the Azores and Atlantic islands are reported for comparison.

(Ba/Nb, Rb/Ta, Th/Ta and LILE/LILE; Fig. 9). Only Rb, Ba and K, to a lesser extent, show greater variations; Ba/Nb and Rb/Ta ratios increase with normative nepheline (Fig. 10). REEs are fractionated for both light REEs (LREEs) and HREEs, but there is variable La/Yb at almost constant Tb_N/Yb_N (~ 1.7–2.0) (Fig. 9f).

Since garnet is one of the few discriminating mantle phases as regards HREEs (i.e. $D_{Tb}^{Gt} = 1.0–1.18$; $D_{Yb}^{Gt} = 5.0–6.25$) (Adam & Green, 2006), the observed HREE fractionation of the Faial basalts can be explained only by the assumption that some garnet was left in the residue during mantle melting. This explanation supports the hypothesis that the magma's parental rock was a garnet peridotite (i.e. $P > 2.8$ GPa; Robinson & Wood, 1998). As confirmation, Beier, Haase & Turner (2012) calculated that melting beneath Faial occurred at $P > 3$ GPa.

According to geochemical modelling by Bourdon, Turner & Ribe (2005), the degree of partial melting in the mantle source for the Azores archipelago can be estimated from the variations of La/Yb versus Tb/Yb. Based on the geochemistry of the most primitive Faial basalts ($\text{MgO} = 7–10$ %), the degree of partial melting for this island would be around 3–5 % for the Horta Fissure Zone and 2–3 % for the Capelo Fissure Zone (Fig. 11), with a slightly higher amount of garnet left during the formation of the Capelo magmas. It should be noted, however, that such a model assumes the existence of a common homogeneous source for all the magmas, while this hypothesis may not be always true, both at a regional scale and even at the level of a single island.

Variable degrees of partial melting of a homogeneous source should also produce a parallel increase in HFSEs

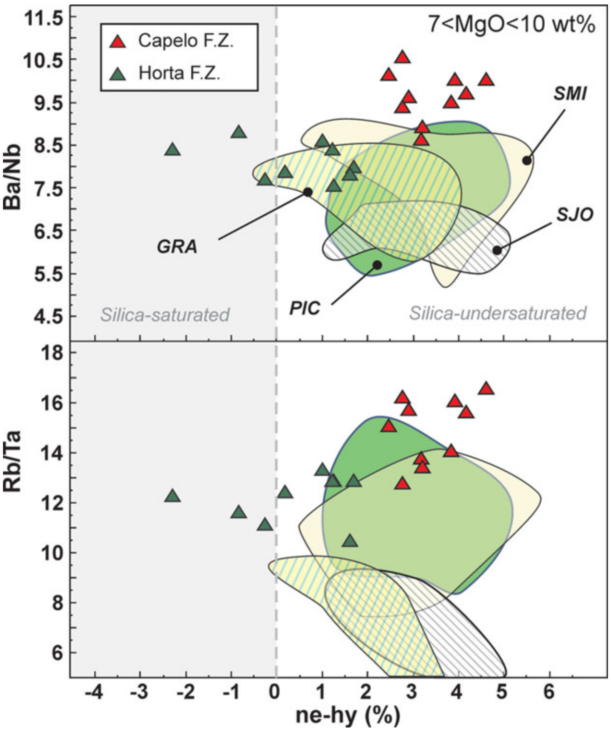

Figure 10. (Colour online) Correlation between the silica saturation (normative ne–hy) and some trace element abundances and ratios for Faial primitive rocks. Fields for the Azorean islands nearby Faial are reported together with São Miguel for comparison and are drawn from literature. All these data are restricted to the MgO interval between 7 and 10 wt %. Acronyms refer to other islands in the Azores and are as follows: SMI – São Miguel; SJO – São Jorge; GRA – Graciosa; PIC – Pico.

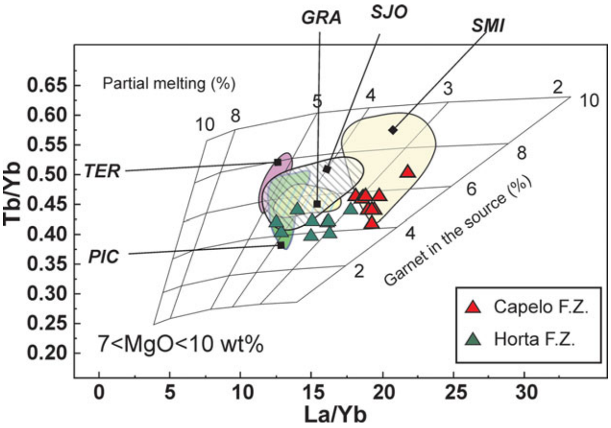

Figure 11. (Colour online) Model of the evaluation of the degree of partial melting versus amount of residual garnet in a primitive garnet-bearing lherzolite source, developed by Bourdon, Turner & Ribe (2005), based upon La/Yb v. Tb/Yb variations. The model assumes fractional melting of a primitive mantle source composition comprising 55 % olivine, 25 % orthopyroxene and variable ratios of clinopyroxene/garnet. SMI – São Miguel; SJO – São Jorge; GRA – Graciosa; PIC – Pico; TER – Terceira Island.

(e.g. Ta, Nb), which are as greatly incompatible with mantle mineralogy as many LILEs and LREEs. This is not observed at Faial, as discussed earlier. Therefore, geochemical evidence argues against variable degrees of partial melting and rather supports the hypothesis that melting originated from a variably LILE-enriched heterogeneous source in the mantle. In effect, this could be connected to various degrees of metasomatic modifications, which heterogeneously enriched the mantle source in LILEs such as Rb, Ba, Na and K, but not in HFSEs. LILEs could have been stored in various hydrous phases (e.g. phlogopite, amphibole; McKenzie & O'Nions, 1991; Zack, Foley & Jenner, 1997), whose breakdown enriched the source in these elements (Melzer & Wunder, 2001).

Mafic rocks from Faial show similar compositions for some elements, but also display important geochemical differences with respect to other Azorean basalts, at a similar range of MgO (7–10 wt %) and SiO_2 (White, Tapia & Schilling, 1979; Turner *et al.* 1997; Widom *et al.* 1997; Claude-Ivanaj, Joron & Allégre, 2001; Beier, Haase & Hansteen, 2006; Beier, Stracke & Hansteen, 2007; Elliott *et al.* 2007; Beier *et al.* 2008; Hildenbrand *et al.* 2008; Prytulak & Elliott, 2009; Millet *et al.* 2009; Madureira *et al.* 2011; Beier, Haase & Turner, 2012). All mafic rocks from the Azores have comparable abundances of HFSEs and HFSE/HFSE ratios. In contrast, they are slightly undersaturated in silica in most islands with moderate amounts of normative nepheline. Unlike at Faial, hy-normative basalts are scarce or absent. LILE abundances are slightly higher at Faial, with some LILE/HFSE displaying notably higher values than at other islands. Overall, the available trace element data indicate some differences in the enrichment mechanisms in the upper mantle beneath Faial, with more intensive degrees of LILE enrichment than in the other islands.

Compared to the islands of Capo Verde, Madeira, the Canary archipelago and St Helena, the LILE/HFSE ratios of Faial (Rb/Ta, Ba/Nb) are generally higher, whereas they are more similar to those of Tristan da Cunha and slightly lower than those of Gough. In contrast, La/Yb and Tb/Yb ratios are generally low (data from the 'georoc database' and references therein: http://georoc.mpch-mainz.gwdg.de/georoc/). However, a detailed discussion on such a complex pattern of element variations is beyond the scope of this paper. It can only be commented that this complexity likely reflects variable degrees of mantle metasomatism and of partial melting in the generation of mafic magmas in these islands. High LILE/HFSE values at Faial highlight important LILE enrichments that suggest a different style of metasomatic modification from that of other Atlantic islands. Such a preferential enrichment is not typical of intraplate environments, and, if confirmed by further detailed studies on other mafic rocks at a regional scale, it would have important implications regarding the mechanism of mantle enrichment beneath the Azores. It would also constitute a constraint on the solution to the dilemma of whether volcanism represents a deep mantle plume or a volatile-enriched mantle (Bonatti, 1990; McKenzie & O'Nions, 1995; Montelli *et al.* 2004; Asimow, Dixon & Langmuir, 2004).

Table 3. Results of mass balance calculations applied to the different magmatic series of the volcanic systems of the island

Initial composition	Final composition	Total added phases (wt %) [*specification and relative amount*]	Total subtracted phases (wt %) [*specification and relative amount*]	Sum of the square of the residuals (χ^2)
Horta Fissure Zone Ne-normative series				
Basalt FYS301	Alkali basalt FYS309	**0**	**21.5** *[pl (39.7), ol (35.8), cpx (24.4)]*	0.215
Horta Fissure Zone Hy-normative series				
Basalt FYS302	Alkali basalt FYS328	**0**	**37** *[Ti-mag (3.0), ol (18.8), pl (34.5), cpx (43.7)]*	0.079
Capelo Fissure Zone Ne-normative series				
Basalt FYS357	Hawaiite FYS347	**0**	**24.5** *[Ti-mag (3.2), ol (35.8), pl (38.4), cpx (22.5)]*	0.250
Caldeira Volcano Ne-normative series				
Alkalibasalt FYS309	Mugearite 1Fa-Ce1	**0**	**35** *[ap (0.5), Ti-mag (4.7), ol (19.1), cpx (25.4), pl (50.3)]*	0.185
Mugearite 1Fa-Ce1	Trachyte FYS-14	**0**	**34.7** *[ol (1.3), ap (4.4), bt (5.0), amp (9.0), Ti-mag (20.3), pl (21.3), cpx (38.8)]*	0.064
Caldeira Volcano Hy-normative series				
Alkali basalt FYS328	Benmoreite FYS321	**0**	**49** *[ap (1.7), Ti-mag (3.7), cpx(7.1), ol (10.6), pl (22.6), amp (54.3)]*	0.293
Benmoreite FYS321	Trachyte FYS-17	**0**	**43** *[bt (1.3), ap (1.4), Ti-mag (3.5), af (26.7), pl (30.7), amp (36.5)]*	0.166
Caldeira Volcano Ba-rich benmoreites				
Benmoreite 1Fa-Ce3	Benmoreite FYS327	**16** *[pl (3.2), ap (7.7), Ti-mag (13.5),] af (22.9), cpx (52.8)]*	**0**	0.137

There are various metasomatic agents invoked to explain the geochemical characteristics of mantle worldwide. Among them, the only one that can cause the variations observed between the two fissure zones (i.e. selective variations in Ba, Rb, Sr, K, LREEs and degree of silica saturation/undersaturation) is an aqueous fluid phase, coexisting or not with silicate melts (e.g. Scambelluri *et al.* 2006). This phase, however, should play a role only at a local scale, as not all the magmas erupted at the Horta Fissure Zone, as an example, show the same characteristics. This particular geochemical signature should be acquired at the moment of melt formation, at the spinel/garnet transition. For this reason, the fluids released by serpentinized oceanic crust at the depth of the Moho can be ruled out. At the same time, it is improbable that these fluids could be provided by the 3 Ga material lying at depth. Lithospheric mantle beneath the Azores is mainly constituted by ultrarefractory lithologies (Simon *et al.* 2008); however, the local presence of hydrous lithologies cannot be fully excluded, and thus their dehydration (phlogopite or amphibole breakdown) could release the necessary fluid (e.g. Coltorti & Gregoire, 2008).

7.b. Magma evolution processes: the role of fractional crystallization

The most primitive magmas of Faial experienced variable degrees of evolution during their ascent to the surface. The comprehension of the processes of magma evolution has important implications for understanding the origin of derivative magmas and for modelling the plumbing system of the volcano. In general, only magmas from the Capelo and Horta fissure zones experienced moderate degrees of fractional crystallization and evolved to hawaiites, whereas the evolution process of the lavas erupted from the Caldeira Volcano continued and completed with the formation of trachytes.

Magma evolution processes were tested both by trace element modelling and mass balance calculations, based on major elements and mineral chemistry (Stormer & Nicholls, 1978), aiming at determining (1) the amount and type of fractionation processes, (2) the nature of crystallizing mineral phases in the different volcanic centres and (3) the conditions of magma storage and fractionation.

Starting from a parent magma with the composition of FYS301, one of the most primitive and sub-aphyric rocks from the Horta Fissure Zone, the formation of the ne-normative alkali basalts of the fissure zones must have required about 20 % removal of Fe-Mg phases plus some plagioclase. A higher amount of fractional crystallization (37 %) of the same phases, plus oxides has been calculated for the hy-normative basalt-to-hawaiite suite (see Table 3 for details). The generation of the hawaiites of the Capelo Fissure Zone required the removal of an amount of mineral phases similar to those of Horta (24.5 %), starting from the least evolved basaltic sample (FYS357) of the series. The most primitive rocks of the Caldeira Volcano are both hy- and ne-normative and show low abundances of MgO and Ni and Cr trace elements (Figs 2, 7). Mass balance calculations suggest that fractional crystallization of mafic phases, titanomagnetite and plagioclase accounts for the formation of the hy-normative alkali basalts of the Caldeira Volcano. An even higher degree of fractionation of these phases, along with amphibole, some biotite, apatite and alkali feldspars, favoured the generation of benmoreite and trachyte magmas (see Table 3 for details). Overall, about 80 % total fractional crystallization is necessary to form trachytes from basaltic parental magmas. The formation of the undersaturated series requires significantly lower amounts (~ 60 %) of fractional crystallization to obtain trachytic compositions. It must be noted, however, that the modelled undersaturated trachytes (FYS14) contain less silica and higher MgO than the modelled oversaturated ones (FYS17) (online Supplementary Data Table S1 at http://journals.cambridge.org/geo).

Samples from the Grupo Inferior, characterized by MgO contents in the range 3–4.4 wt %, show anomalously high Al_2O_3, CaO and Sr contents. While Al_2O_3 is negatively correlated with MgO, the contents of the other two elements show a positive correlation. These variations are linked to the accumulation of plagioclase in these rocks. Other samples of the Grupo Inferior, especially the most evolved ones, show high Ba contents and a small but significant positive Eu anomaly in REE patterns. These two parameters are positively correlated with each other (not shown). In particular, two benmoreites show very high Ba content (exceeding 1130 ppm), which is not linked to any other chemical parameter. These rocks contain a few alkali feldspar phenocrysts with disequilibrium features, indicating that the high Ba content is related to the accumulation of alkali feldspar.

The variation of trace elements is more sensitive to evolution processes and can provide further constraints on the model. Figure 12 shows the variation diagrams of Sr v. Ba and La/Yb v. Zr. Barium-rich (cumulated) samples have been excluded from the Ba–Sr plot, in which three different trends may be distinguished (Fig. 12a). A positive trend (trend 1) is defined by the bulk of mafic rocks, when fractionation is dominated by mafic phases, and both Ba and Sr are incompatible. It is notable, however, that some original variations of the primitive magmas also superimpose over this trend. A negative trend is observed for intermediate compositions when plagioclase becomes an important fractionating phase and Sr, but not Ba, becomes compatible (trend 2). Finally, both Ba and Sr decrease towards trachytic composition when both alkali feldspar and plagioclase become dominant fractionating phases (trend 3). This is in agreement with the results of mass balance calculations.

Various trends are also present in the plot where the ratios of elements with a different degree of incompatibility, such as La and Yb, are plotted against an incompatible element such as Zr (Fig. 12b). Poorly evolved compositions show limited variations of Zr, as compared to the values of the La/Yb ratio. As discussed in the previous section, this is an effect of the partial melting of sources with different degrees of metasomatism (i.e. variable enrichments in LREEs and LILEs), followed by little degrees of fractional crystallization. The other two trends regarding the evolved rocks indicate separation of different phenocrysts during fractional crystallization. A positive trend in Zr v. La/Yb, which is mostly formed by intermediate rocks of the Caldeira Volcano, requires the fractional crystallization of mainly clinopyroxene. The other trend, which shows poorly variable La/Yb at variable Zr, can be modelled by about 80 % fractional crystallization, dominated by separation of feldspars.

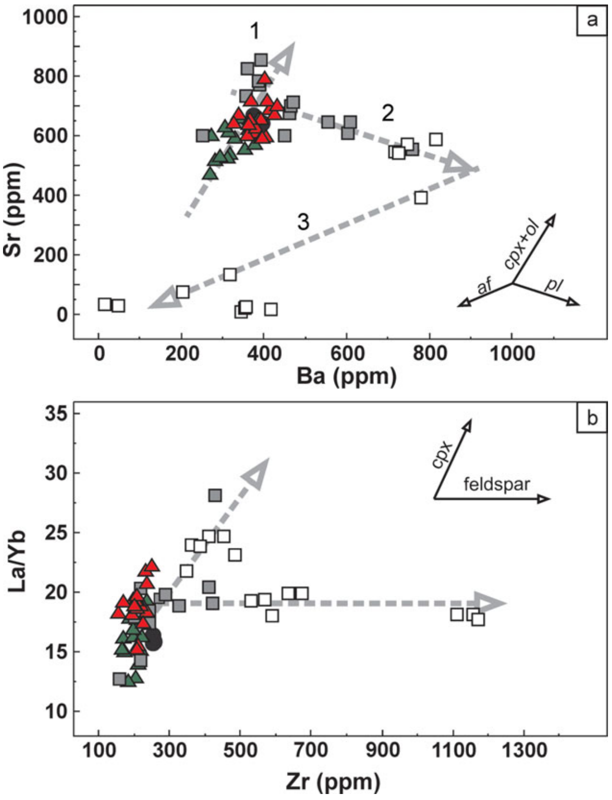

Figure 12. (Colour online) Trace element models of fractional crystallization for the Faial volcanic products. Rocks that suffered from the accumulation of either mafic phases or feldspar are not reported. Element variations caused by the fractionation of the main mineral phases are indicated by arrows in the insets.

7.c. Modelling of the storage and feeding system

The petrological and geochemical modelling of the magma evolution discussed above may aid in the comprehension of the dynamics governing magma ascent and storage at Faial Island and provide important indications about the structure of the plumbing system, both along the fissure zones and at the central volcano. The main steps regarding magma generation and evolution at Faial consist of (i) low degrees of partial melting of a variably metasomatized upper mantle in the garnet facies (> 85–90 km deep; Robinson & Wood, 1998); (ii) moderate degrees of fractional crystallization beneath the areas of the Horta and Capelo fissure zones, with the formation of hawaiites; and (iii) high degrees of fractional crystallization beneath the Caldeira Volcano, with the formation of benmoreites and trachytes.

Geobarometric data for basalts and hawaiites from the Horta and Capelo fissure zones (Table 2), suggest high to intermediate pressures of crystallization, corresponding to the uppermost mantle (~ 15 to 28 km). This is shallower than the zone of magma origin of basalts, located at a depth ranging on average from 3.1 to 3.4 GPa (Beier, Haase & Turner, 2012), in the garnet peridotite facies (~ 100 to 110 km). However, primitive crystals formed at pressures greater than 1 GPa. A polybaric crystallization is also suggested by Al^{IV}/Al^{VI}–Si–Ti variation for clinopyroxenes only for the Capelo Fissure Zone and the central volcano (Fig. 5). These pressures are higher than the stability field of plagioclase, which explains the absence of this phase as a phenocryst in many rocks, including ankaramites, as well as the incompatible behaviour of Sr during fractionation of these magmas. The poorly variable and generally high Al^{IV}/Al^{VI} values in lavas from the Horta Fissure Zone suggest that clinopyroxene crystallization occurred at a shallower depth than for the other sites.

Hawaiites rose from storage areas located at the boundary between the crust and mantle and erupted through fractures that followed the regional trend. The crystallization of plagioclase and magnetite-ilmenite microlites in these rocks probably occurred during water degassing in shallow feeder dykes prior to eruption, producing the characteristic intersertal texture of these lavas. The low degree of evolution of the lavas erupted at the Horta and Capelo fissure zones indicates a lack or minor degree of magma ponding and associated crystallization within the crust.

As regards the Caldeira Volcano, hy-normative basalts, similar in composition to those of the Horta Fissure Zone, equilibrated at 760 MPa (~ 26 km) beneath the present edifice, until the probable generation of a Sr-rich mugearite–benmoreite series at 159 MPa (~ 9 km). A Sr-poor benmoreite–trachyte series formed after the ~ 70 % fractionation of mafic phases, biotite, apatite and feldspars in a reservoir possibly located at a depth of 100–132 MPa (~ 3.5–5 km). Possibly, this ponding level indicates that the conditions of neutral buoyancy for these magmas were matched, owing to a sudden jump in density of the country rocks. This jump may be related to the shift from hydrothermalized MORB-type basalts, ~ 15 Ma (Müller *et al.* 2008), to the younger (~ 3–10 Ma; Cannat *et al.* 1999; Escartín *et al.* 2001; Maia, Goslin & Gente, 2007) and denser basaltic rocks of the Azores Plateau. A schematic petrology-based model of the plumbing system of Faial is outlined in Figure 13.

8. Conclusions

The Island of Faial was built by mostly lavas and subordinate pyroclastic rocks ranging in composition from basalt to trachyte. Eruptions of mafic magmas occurred along the fissure zones of Capelo and Horta. A suite of rocks of basaltic to trachytic composition built up the Caldeira Volcano starting from about 120 ka ago. Emission of trachytes started about 16 ka ago, when the two fissure zones also began their activity.

Mafic magmas range from silica-saturated to moderately silica-undersaturated. They show a positive correlation between normative nepheline and many LILE abundances and LILE/HFSE ratios. Geochemical evidence excludes the hypothesis that these correlations are the result of fractional crystallization and rather suggests that mantle-equilibrated parental magmas were generated in a heterogeneous source that had undergone variable degrees of metasomatism. Such a process generated variable enrichments in LILEs, but not in other incompatible elements such as HFSE (Nb, Ta, etc).

Mafic magmas underwent fractional crystallization beneath the fissure zones and the Caldeira Volcano. Moderate degrees of polybaric fractionation in deep magma reservoirs beneath the Capelo Fissure Zone generated the basalt-to-hawaiite magmas, which directly fed the eruptions at this zone. In the case of the Horta Fissure Zone, fractional crystallization occurred at a shallower depth to generate magmas with a similar degree of evolution as the Capelo Fissure Zone. Polybaric fractional crystallization at shallower depths beneath Caldeira led to the formation of basalt-to-benmoreite and trachyte series, with silica increasing over time.

The space and time distribution of volcanic activity in Faial, coupled with the variation of petrological and geochemical features of the erupted products, can be summarized in a conceptual model of the internal structure of the island, as already attempted for several other active volcanic systems (e.g. Vulcano Island, Italy; Zanon, Frezzotti & Peccerillo, 2003; Peccerillo *et al.* 2006). According to the proposed model, the slightly undersaturated to saturated parental magmas evolved by fractional crystallization in the uppermost mantle, producing a hawaiite suite. These magmas reached the surface without significant stagnation and erupted along the two fissure zones. On the contrary, more complex evolution processes took place beneath the Caldeira Volcano, producing a suite of basalt-to-trachyte melts. Geochemical and petrological data indicate a polybaric fractionation of these magmas, and suggest the possible existence of reservoirs at different depths within the crust. The main emission of evolved magmas during the latest stages of Caldeira activity suggests that the eruptions tapped the shallower magma chambers where evolution had generated trachytic melts. The lack of ponding areas for basaltic-hawaiitic magmas in the crust may depend on the presence of a density filter at the base of the Moho. The presence of ultramafic cumulitic levels in the lithospheric mantle at the base of the crust could act as a density filter, stopping ascending magmas and favouring their accumulation (underplating) and the subsequent fractionation. This phenomenon has already been reported for the volcanoes of the Canary Islands and Madeira (Dañobeitia & Canales, 2000; Schwarz, Klügel & Wohlgemuth-Ueberwasser, 2004; Klügel, Hansteen & Galipp, 2005) and therefore would not constitute a new finding in the framework of the oceanic islands of this area of the Atlantic Ocean.

The variable behaviour of magmas during their ascent beneath the central volcano and the rift zones

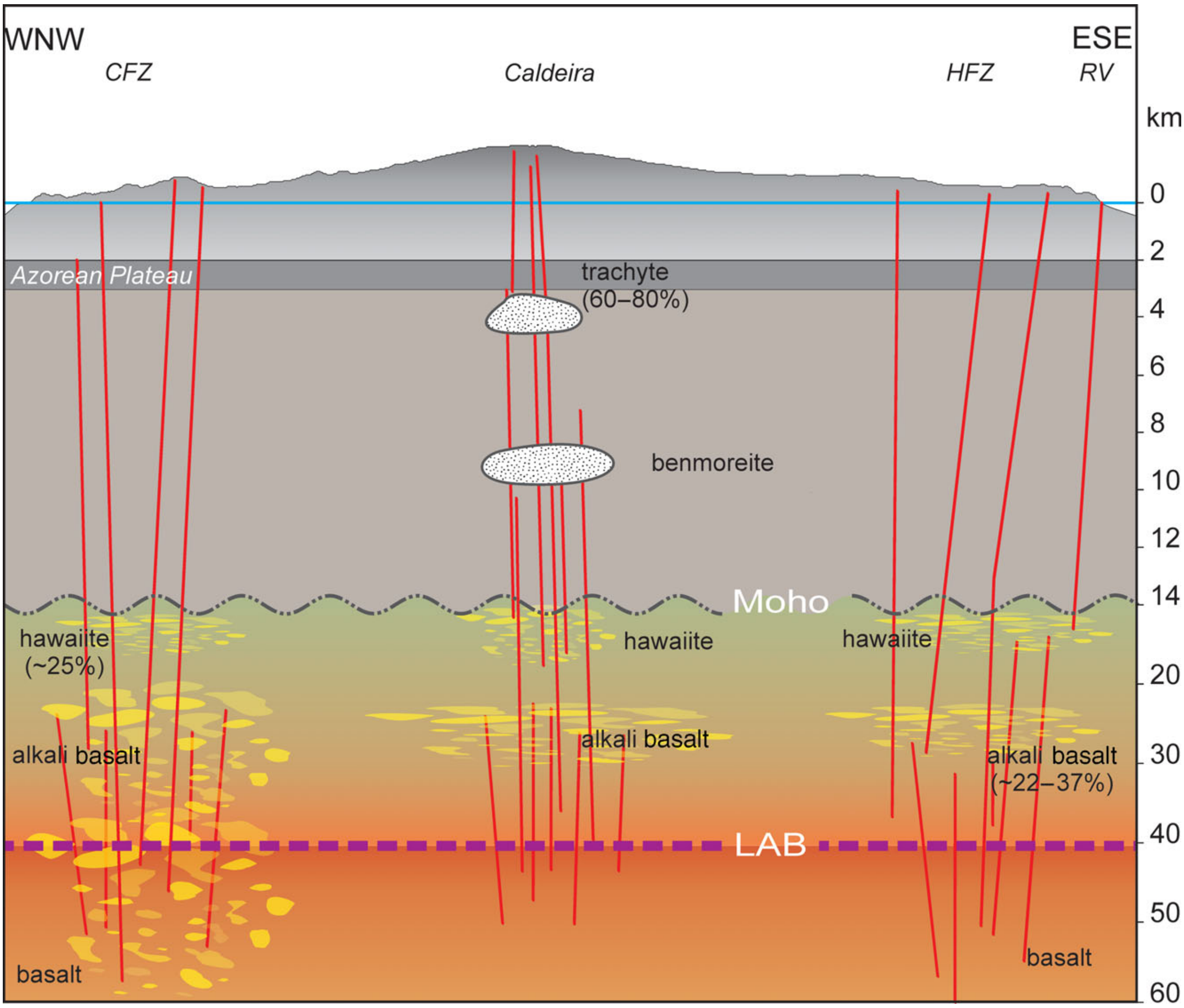

Figure 13. (Colour online) Schematic model along a WNW–ESE direction of a magma ascent path and the conduit systems feeding the various volcanic complexes. Total degree of fractional crystallization and magma compositions are reported for clarity. The boundary with the mantle is from Dias *et al*. (2007). Lithosphere–asthenosphere boundary (LAB) is from Féraud, Kaneoka & Allègre (1980). Abbreviations: CFZ – Capelo Fissure Zone; HFZ – Horta Fissure Zone; RV – Ribeirinha Volcano.

could have been the result of different local conditions of the tectonic stress. Fissure volcanism developed along extensional WNW- and ESE-trending fissures, whereas the central volcano formed at the intersection between those faults and the NNW–SSE transtensional systems. In such a tectonic setting, the formation of magma reservoirs was favoured and trachytic magmas were formed.

Acknowledgements. This work has been funded by the Direcção Regional da Ciência e Tecnologia (DRCT – medida M2.1.2/004/2007 and programme RAA/DRCT). A. Risplendente and S. Poli of the Earth Sciences Department of the ‘Ardito Desio’ University of Milan (Italy) are gratefully acknowledged for their assistance during microprobe analyses. Thanks are also extended to R. Coutinho, who provided help during fieldwork. Discussions with C. Beier and criticisms from two anonymous reviewers proved very useful and contributed to the improvement of the manuscript.

References

ACOCELLA, V. & NERI, M. 2003. What makes flank eruptions? The 2001 Etna eruption and its possible triggering mechanisms. *Bulletin of Volcanology* **65**, 517–29.

ADAM, J. & GREEN, T. 2006. Trace element partitioning between mica- and amphibole-bearing garnet lherzolite and hydrous basanitic melt: 1. Experimental results and the investigation of controls on partitioning behaviour. *Contributions to Mineralogy and Petrology* **152**, 1–17.

ANDERSEN, D. J. & LINDSLEY, D. H. 1985. New (and final) models for the Ti-magnetite/ilmenite geothermometer and oxygen barometer. *Abstracts of the American Geophysical Union 1985 Spring Meeting, EOS* **66**, 416.

ANDERSEN, D. J., LINDSLEY, D. H. & DAVIDSON, P. M. 1993. QUILF: a Pascal program to assess equilibria among Fe-Mg-Mn-Ti oxides, pyroxenes, olivine, and quartz. *Computers and Geosciences* **19**, 1333–50.

ASIMOW, P. D., DIXON, J. E. & LANGMUIR, C. H. 2004. A hydrous melting and fractionation model for mid-ocean ridge basalts: application to the Mid-Atlantic Ridge near the Azores. *Geochemistry, Geophysics, Geosystems* **5**, Q01E16, doi: 10.1029/2003GC000568.

Beier, C., Haase, K. M., Abouchami, W., Krienitz, M.-S. & Hauff, F. 2008. Magma genesis by rifting of oceanic lithosphere above anomalous mantle: Terceira Rift, Azores. *Geochemistry, Geophysics, Geosystems* **9**, Q12013, doi: 10.1029/2008GC002112.

Beier, C., Haase, K. M. & Hansteen, T. H. 2006. Magma evolution of the Sete Cidades volcano, São Miguel, Azores. *Journal of Petrology* **47**, 1375–411.

Beier, C., Haase, K. M. & Turner, S. P. 2012. Conditions of melting beneath the Azores. *Lithos* **144–145**, 1–11.

Beier, C., Stracke, A. & Haase, K. M. 2007. The peculiar geochemical signatures of São Miguel (Azores) lavas: metasomatised or recycled mantle sources? *Earth and Planetary Science Letters* **259**, 186–99.

Bonatti, E. 1990. Not so hot "hot spots" in the oceanic mantle. *Science* **250**, 107–11.

Borgia, A., Ferrari, L. & Pasquarè, G. 1992. Importance of gravitational spreading in the tectonic and volcanic evolution of Mt. Etna. *Nature* **357**, 231–5.

Borgia, A. 1994. Dynamic basis of volcanic spreading. *Journal of Geophysical Research* **99**, 17791–804.

Bourdon, B., Turner, S. P. & Ribe, N. M. 2005. Partial melting and upwelling rates beneath the Azores from a U-series isotope perspective. *Earth and Planetary Science Letters* **239**, 42–56.

Cannat, M., Briais, A., Deplus, C., Escartín, J., Georgen, J., Lin, J., Mercouriev, S., Meyzen, C., Muller, M., Pouliquen, G., Rabain, A. & Da Silva, P. 1999. Mid-Atlantic Ridge–Azores hotspot interactions: along-axis migration of a hotspot-derived event of enhanced magmatism 10 to 4 Ma ago. *Earth and Planetary Science Letters* **173**, 257–69.

Civile, D., Lodolo, E., Tortorici, L., Lanzafame, G. & Brancolini, G. 2008. Relationships between magmatism and tectonics in a continental rift: the Pantelleria Island region (Sicily Channel, Italy). *Marine Geology* **251**, 32–46.

Claude-Ivanaj, C., Joron, J. L. & Allègre, C. J. 2001. ^{238}U–^{230}Th–^{226}Ra fractionation in historical lavas from the Azores: long-lived source heterogeneity vs. metasomatism fingerprints. *Chemical Geology* **176**, 295–310.

Coltorti, M. & Gregoire, M. 2008. Metasomatism in oceanic and continental lithospheric mantle: introduction. In *Metasomatism in Oceanic and Continental Lithospheric Mantle* (eds M. Coltorti & M. Gregoire), pp. 1–9. Geological Society of London, Special Publication no. 293.

Corsaro, R. A., Métrich, N., Allard, P., Andronico, D., Miraglia, L. & Fourmentraux, C. 2009. The 1974 flank eruption of Mount Etna: an archetype for deep dike-fed eruptions at basaltic volcanoes and a milestone in Etna's recent history. *Journal of Geophysical Research* **114**, B07204, doi:10.1029/2008JB006013.

Corsaro, R. A. & Pompilio, M. 2004. Magma dynamics in the shallow plumbing system of Mt. Etna as recorded by compositional variations in volcanics of recent summit activity (1995–1999). *Journal of Volcanology and Geothermal Research* **137**, 55–71.

Dañobeitia, J. J. & Canales, J. P. 2000. Magmatic underplating in the Canary Archipelago. *Journal of Volcanology and Geothermal Research* **103**, 27–41.

Davidson, J. P., Morgan, D. J., Charlier, B. L. A., Harlou, R. & Hora, J. M. 2007. Microsampling and isotopic analysis of igneous rocks: implications for the study of magmatic systems. *Annual Review of Earth and Planetary Sciences* **35**, 273–311.

Dias, N. A., Matias, L., Lourenço, N., Madeira, J., Carrilho, F. & Gaspar, J. L. 2007. Crustal seismic velocity structure near Faial and Pico Islands (AZORES), from local earthquake tomography. *Tectonophysics* **445**, 301–31.

Donaldson, C. H. 1976. An experimental investigation of olivine morphology. *Contributions to Mineralogy and Petrology* **57**, 187–213.

Elliott, T., Blichert-Toft, J., Heumann, A., Koetsier, G. & Forjaz, V. H. 2007. The origin of enriched mantle beneath São Miguel, Azores. *Geochimica et Cosmochimica Acta* **71**, 219–40.

Escartín, J., Cannat, M., Pouliquen, G., Rabain, A. & Lin, J. 2001. Crustal thickness of V-shaped ridges south of the Azores: interaction of the Mid-Atlantic Ridge (36°–39°N) and the Azores hot spot. *Journal of Geophysical Research* **106**, B10, 21719–21735, doi: 10.1029/2001JB000224.

Féraud, G., Kaneoka, I. & Allègre, C. J. 1980. K/Ar ages and stress pattern in the Azores: geodynamic implications. *Earth and Planetary Science Letters* **46**, 275–86.

França, Z. T. M., Tassinari, C. C. G., Cruz, J. V., Aparicio, A. Y., Araña, V. & Rodrigues, B. N. 2006. Petrology, geochemistry and Sr–Nd–Pb isotopes of the volcanic rocks from Pico Island – Azores (Portugal). *Journal of Volcanology and Geothermal Research* **156**, 71–89.

Garcia, M. O., Pietruszka, A. J., Rhodes, J. M. & Swanson, K. 2000. Magmatic processes during the prolonged Pu'u 'O'o eruption of Kilauea volcano, Hawaii. *Journal of Petrology* **41**, 967–90.

Green, D. H. & Ringwood, A. E. 1976. The genesis of basaltic magmas. *Contributions to Mineralogy and Petrology* **15**, 103–90.

Gupta, A. K., Green, D. H. & Taylor, W. R. 1987. The liquidus surface of the system forsterite-nepheline-silica at 28 kb. *American Journal of Science* **287**, 560–5.

Hildenbrand, A., Madureira, P., Ornelas Marques, F., Cruz, I., Henry, B. & Silva, P. 2008. Multi-stage evolution of a sub-aerial volcanic ridge over the last 1.3 Myr: S. Jorge Island, Azores Triple Junction. *Earth and Planetary Science Letters* **273**, 289–98.

Hildenbrand, A., Marques, F. O., Costa, A. C. G., Sibrant, A. L. R., Silva, P. F., Henry, B., Miranda, J. M. & Madureira, P. 2012. Reconstructing the architectural evolution of volcanic islands from combined K/Ar, morphologic, tectonic, and magnetic data: the Faial Island example (Azores). *Journal of Volcanology and Geothermal Research* **241–242**, 39–48.

Irvine, T. N. & Baragar, W. R. A. 1971. A guide to the chemical classification of the common volcanic rocks. *Canadian Journal of Earth Sciences* **8**, 523–48.

Klügel, A., Hansteen, T. H. & Galipp, K. 2005. Magma storage and underplating beneath Cumbre Vieja volcano, La Palma (Canary Islands). *Earth and Planetary Science Letters* **236**, 211–26.

Lacasse, C., Sigurdsson, H., Carey, S. N., Jóhannesson, H., Thomas, L. E. & Rogers, N. W. 2007. Bimodal volcanism at the Katla subglacial caldera, Iceland: insight into the geochemistry and petrogenesis of rhyolitic magmas. *Bulletin of Volcanology* **69**, 373–99.

Macdonald, G. A. 1968. Composition and origin of Hawaiian lavas. *Geological Society of America Memoir* **116**, 477–522.

Machado, F., Parsons, W. H., Richards, A. F. & Mulford, J. W. 1962. Capelinhos eruption of Fayal

Volcano, Azores. *Journal of Geophysical Research* **67**, 3519–29.

Madeira, J. & Silveira, A. B. 2003. Active tectonics and first paleoseismological results in Faial, Pico and S. Jorge Islands (Azores, Portugal). *Annals of Geophysics* **46**, 733–61.

Madureira, P., Mata, J., Mattielli, N., Queiroz, G. & Silva, P. 2011. Mantle source heterogeneity, magma generation and magmatic evolution at Terceira Island (Azores archipelago): constraints from elemental and isotopic (Sr, Nd, Hf, and Pb) data. *Lithos* **126**, 402–18.

Maia, M., Goslin, J. & Gente, P. 2007. Evolution of the accretion processes along the Mid-Atlantic Ridge north of the Azores since 5.5 Ma: an insight into the interactions between the ridge and the plume. *Geochemistry, Geophysics, Geosystems* **8**, Q03013, doi: 10.1029/2006GC001318, 19 pp.

McDonough, W. F. & Sun, S. S. 1995. The composition of the Earth. *Chemical Geology* **120**, 223–53.

McKenzie, D. A. N. & O'Nions, R. K. 1991. Partial melt distributions from inversion of rare Earth element concentrations. *Journal of Petrology* **32**, 1021–91.

McKenzie, D. A. N. & O'Nions, R. K. 1995. The source regions of Ocean Island Basalts. *Journal of Petrology* **36**, 133–59.

Melzer, S. & Wunder, B. 2001. K-Rb-Cs partitioning between phlogopite and fluid: experiments and consequences for the LILE signatures of island arc basalts. *Lithos* **59**, 69–90.

Métrich, N., Bizouard, H. & Varet, J. 1981. Petrology of the volcanic series of Fayal, Azores. *Bulletin Volcanologique* **44**, 71–93.

Millet, M. A., Doucelance, R., Baker, J. A. & Schiano, P. 2009. Reconsidering the origins of isotopic variations in Ocean Island Basalts: insights from fine-scale study of São Jorge Island, Azores archipelago. *Chemical Geology* **265**, 289–302.

Montelli, R., Nolet, G., Dahlen, F. A., Masters, G., Engdahl, E. R. & Hung, S. H. 2004. Finite-frequency tomography reveals a variety of plumes in the mantle. *Science* **303**, 338–43.

Moreira, M., Doucelance, R., Dupré, B. & Allègre, C. J. 1999. Helium and lead isotope geochemistry in the Azores. *Earth and Planetary Science Letters* **169**, 189–205.

Morimoto, N. 1989. Nomenclature of pyroxenes. *Canadian Mineralogist* **27**, 143–56.

Müller, R. D., Sdrolias, M., Gaina, C. & Roest, W. R. 2008. Age, spreading rates, and spreading asymmetry of the world's ocean crust. *Geochemistry, Geophysics, Geosystems* **9**, Q04006, doi: 10.1029/2007GC001743, 19 pp.

Münn, S., Walter, T. R. & Klügel, A. 2006. Gravitational spreading controls rift zones and flank instability on El Hierro, Canary Islands. *Geological Magazine* **143**, 257–68.

O'Hara, M. J. 1968. The bearing of phase equilibria studies in synthetic and natural systems on the origin and evolution of basic and ultrabasic rocks. *Earth-Science Reviews* **4**, 69–133

Pacheco, J. M. 2001. *Processos associados ao desenvolvimento de erupções vulcânicas hidromagmáticas na Ilha do Faial e sua interpretação numa perspectiva de avaliação do hazard e minimização do risco*. Ph.D. thesis, Departamento de Geociências, Ponta Delgada: Universidade dos Açores. Published thesis.

Peccerillo, A., Barberio, M. R., Yirgu, G., Ayalew, D., Barbieri, M. & Wu, T. W. 2003. Relationships between mafic and peralkaline silicic magmatism in continental rift settings: a petrological, geochemical and isotopic study of the Gedemsa volcano, central Ethiopian Rift. *Journal of Petrology* **44**, 2003–32.

Peccerillo, A., Donati, C., Santo, A. P., Orlando, A., Yirgu, G. & Ayalew, D. 2007. Petrogenesis of silicic peralkaline rocks in the Ethiopian Rift: geochemical evidence and volcanological implications. *Journal of African Earth Sciences* **48**, 161–73.

Peccerillo, A., Frezzotti, M. L., De Astis, G. & Ventura, G. 2006. Modelling the magma plumbing system of Vulcano (Aeolian Islands, Italy) by integrated fluid-inclusions geobarometry, petrology and geophysics. *Geology* **34**, 17–20.

Prytulak, J. & Elliott, T. 2009. Determining melt productivity of mantle sources from ^{238}U-^{230}Th and ^{235}U-^{231}Pa disequilibria; an example from Pico Island, Azores. *Geochimica et Cosmochimica Acta* **73**, 2103–22.

Putirka, K. 2008. Thermometers and barometers for volcanic systems. In *Minerals, Inclusions and Volcanic Processes* (eds K. Putirka & F. Tepley), pp. 61–120. Reviews in Mineralogy and Geochemistry 69. Mineralogical Society of America.

Ridolfi, F. & Renzulli, A. 2012. Calcic amphiboles in calc-alkaline and alkaline magmas: thermobarometric and chemometric empirical equations valid up to 1,130°C and 2.2 GPa. *Contributions to Mineralogy and Petrology* **163**, 877–95.

Robinson, J. A. C. & Wood, B. J. 1998. The depth of the spinel to garnet transition at the peridotite solidus. *Earth and Planetary Science Letters* **164**, 277–84.

Ryan, M. P., Koyanagi, R. Y. & Fiske, R. S. 1981. Modeling the three dimensional structure of macroscopic magma transport systems: application to Kilauea Volcano, Hawaii. *Journal of Geophysical Research* **86**, 7111–29.

Scambelluri, M., Herman, J., Morten, L. & Rampone, E. 2006. Melt- versus fluid-induced metasomatism in spinel to garnet wedge peridotites (Ulten Zone, Eastern Italian Alps): clues from trace element and Li abundances. *Contributions to Mineralogy and Petrology* **151**, 372–94.

Schaefer, B. F., Turner, S., Parkinson, I., Rogers, N. & Hawkesworth, C. 2002. Evidence for recycled Archaean oceanic mantle lithosphere in the Azores plume. *Nature* **420**, 304–7.

Schilling, J. G., Bergeron, M. B. & Evans, R. 1980. Halogens in the mantle beneath the North Atlantic. *Philosophical Transactions of the Royal Society of London* **297**, 147–78.

Schwarz, S., Klügel, A. & Wohlgemuth-Ueberwasser, C. 2004. Melt extraction pathways and stagnation depths beneath the Madeira and Desertas rift zones (NE Atlantic) inferred from barometric studies. *Contributions to Mineralogy and Petrology* **147**, 228–40.

Searle, R. 1980. Tectonic pattern of the Azores spreading centre and triple junction. *Earth and Planetary Science Letters* **51**, 415–34.

Simon, N. S. C., Neumann, E. R., Bonadiman, C., Coltorti, M., Delpech, G., Gregoire, M. & Widom, E. 2008. Ultra-refractory domains in the oceanic mantle lithosphere sampled as mantle xenoliths at ocean islands. *Journal of Petrology* **49**, 1223–51.

Storey, M. 1981. Trachytic pyroclastics from Água de Pau volcano, São Miguel, Azores: evolution of a magma body over 4,000 years. *Contributions to Mineralogy and Petrology* **78**, 423–32.

STORMER, J. C. & NICHOLLS, J. 1978. XLFRAC: a program for the interactive testing of magmatic differentiation models. *Computers & Geosciences* **4**, 143–59.

TURNER, S., HAWKESWORTH, C., ROGERS, N. & KING, P. 1997. U-Th isotope disequilibria and ocean island basalt generation in the Azores. *Chemical Geology* **139**, 145–64.

TURNER, S., TONARINI, S., BINDEMAN, I., LEEMAN, W. P. & SCHAEFER, B. F. 2007. Boron and oxygen isotope evidence for recycling of subducted components over the past 2.5 Gyr. *Nature* **447**, 702–5.

VOGT, P. R. & JUNG, W. Y. 2004. The Terceira Rift as hyper-slow, hotspot-dominated oblique spreading axis: a comparison with other slow-spreading plate boundaries. *Earth and Planetary Science Letters* **218**, 77–90.

WALTER, T. R., KLÜGEL, A. & MÜNN, S. 2006. Gravitational spreading and formation of new rift zones on overlapping volcanoes. *Terra Nova* **18**, 26–33.

WASS, S. Y. 1979. Multiple origins of clinopyroxenes in alkali basaltic rocks. *Lithos* **12**, 115–32.

WHITE, W. M., TAPIA, M. D. M. & SCHILLING, J. G. 1979. The petrology and geochemistry of the Azores Islands. *Contributions to Mineralogy and Petrology* **69**, 201–13.

WIDOM, E., CARLSON, R. W., GILL, J. B. & SCHMINCKE, H.-U. 1997. Th–Sr–Nd–Pb isotope and trace element evidence for the origin of the São Miguel, Azores, enriched mantle source. *Chemical Geology* **140**, 49–68.

WIDOM, E. & SHIREY, S. B. 1996. Os isotope systematics in the Azores: implications for mantle plume sources. *Earth and Planetary Science Letters* **142**, 451–65.

ZACK, T., FOLEY, S. F. & JENNER, G. A. 1997. A consistent partition coefficient set for clinopyroxene, amphibole and garnet from laser ablation microprobe analysis of garnet pyroxenites from Kakanui, New Zealand. *Neues Jahrbuch fur Mineralogie-Abhandlungen* **172**, 23–41.

ZANON, V., FREZZOTTI, M. L. & PECCERILLO, A. 2003. Magmatic feeding system and crustal magma accumulation beneath Vulcano Island (Italy): evidence from fluid inclusions in quartz xenoliths. *Journal of Geophysical Research* **108**, 2298–310.